Heliyon 9 (2023) e20100

Contents lists available at ScienceDirect

Heliyon

journal homepage: www.cell.com/heliyon

Chemico-pharmacological and computational studies of *Ophiorrhiza fasciculata* D. Don and *Psychotria silhetensis* Hook. f. focusing cytotoxic, thrombolytic, anti-inflammatory, antioxidant, and antibacterial properties

Parisa Tamannur Rashid [a,b], Md Jamal Hossain [a,c,*], Miss Sharmin Zahan [c], Choudhury Mahmood Hasan [a], Mohammad A. Rashid [a], Muhammad Abdullah Al-Mansur [d], Mohammad Rashedul Haque [a,**]

[a] *Phytochemical Research Laboratory, Department of Pharmaceutical Chemistry, Faculty of Pharmacy, University of Dhaka, Dhaka 1000, Bangladesh*
[b] *Department of Pharmacy, East West University, Dhaka, Bangladesh*
[c] *Department of Pharmacy, State University of Bangladesh, 77 Satmasjid Road, Dhanmondi, Dhaka 1205, Bangladesh*
[d] *Bangladesh Council of Scientific and Industrial Research (BCSIR), Dr. Qudrat-I-Khuda Road, Dhanmondi, Dhaka-1205, Bangladesh*

ARTICLE INFO

Keywords:
Ophiorrhiza fasciculata
Psychotria silhetensis
Antibacterial
Antioxidant
Cytotoxicity
Membrane stabilizing
Thrombolytic
In silico
ADMET
Drug likeliness

ABSTRACT

The current study sought to examine the pharmacological potentials of crude methanolic extracts of *Ophiorrhiza fasciculata* and *Psychotria silhetensis*, as well as their various solvent fractionates, with a focus on cytotoxic, thrombolytic, membrane stabilizing, antioxidant, and antibacterial activities via *in vitro* and *in silico* approaches. The extensive chromatographic and spectroscopic analyses confirmed and characterized two compounds as (±)-licarin B (**1**) and stigmasterol (**2**) from *O. fasciculata* and *P. silhetensis*, respectively. Petroleum ether soluble fraction of *O. fasciculata* and the aqueous soluble fraction of *P. silhetensis* showed the lowest 50% lethal concentrations (1.41 and 1.94 μg/mL, respectively) in brine shrimp bioassay. Likewise, petroleum ether soluble fraction of *O. fasciculata* and aqueous soluble fraction of *P. silhetensis* showed the highest thrombolytic activity with 46.66% and 50.10% lyses of the clot, respectively. The methanol and dichloromethane soluble fractions of *O. fasciculata* reduced erythrocyte hemolysis by 64.03% and 37.08%, respectively, under hypotonic and heat-induced conditions, compared to 81.97% and 42.12% for standard acetylsalicylic acid. In antioxidant activity test, aqueous soluble fraction *O. fasciculata* (IC_{50} = 7.22 μg/mL) revealed promising antioxidant potentialities in comparison to standard butylated hydroxytoluene (IC_{50} = 21.20 μg/mL). In antibacterial screening, chloroform, and dichloromethane soluble fractions of *P. silhetensis* showed a mild antibacterial activity compared with the standard drug ciprofloxacin. Additionally, the molecular docking study corroborated the current *in vitro* findings, and the isolated two constituents had higher binding affinities toward epidermal growth factor receptor, tissue plasminogen activator, vFLIP-IKK gamma stapled peptide dimer, glutathione reductase, and dihydrofolate reductase enzyme than their corresponding standard drugs. In addition, the both isolated compounds exerted favorable pharmacokinetics (absorption, distribution, metabolism, excretion) and toxicological profiles

* Corresponding author. Department of Pharmacy, State University of Bangladesh, 77 Satmasjid Road, Dhanmondi, Dhaka 1205, Bangladesh.
** Corresponding author. Department of Pharmaceutical Chemistry, Faculty of Pharmacy, University of Dhaka, Dhaka 1000, Bangladesh.
E-mail addresses: jamal.du.p48@gmail.com, jamalhossain@sub.edu.bd (M.J. Hossain), haquemr@du.ac.bd (M.R. Haque).

https://doi.org/10.1016/j.heliyon.2023.e20100
Received 3 December 2022; Received in revised form 21 August 2023; Accepted 12 September 2023
Available online 13 September 2023
2405-8440/© 2023 The Authors. Published by Elsevier Ltd. This is an open access article under the CC BY-NC-ND license (http://creativecommons.org/licenses/by-nc-nd/4.0/).

with drug-like qualities in computational-based ADMET and drug likeliness analyses. The current research suggests that both plants have potential as a natural treatment for treating thrombosis, inflammation, and oxidative stress. However, more thorough research is required to thoroughly screen for phytochemicals and pinpoint the precise mechanisms of action of the bioactive metabolites derived from these plants against a broad range of molecular targets.

1. Introduction

Throughout history, medicinal plants have been utilized to treat illnesses and preserve health. Because of the adverse effects of conventional medicines and the rising need for more natural products free of toxins, natural products and alternative therapies have attracted more and more attention over the years [1–3]. The use of natural products and herbal extracts for treating human diseases and disorders has finally started to receive scientific support through experimental and clinical studies [4–6]. According to the World Health Organization (WHO), most developing nations, especially those in Asia, Africa, Latin America, and the Middle East, use traditional medicine, including herbal remedies, to meet their citizens' healthcare needs and concerns [7–9].

Traditional remedies such as herbs are used by over 80% of the people for their daily needs in developing countries [10]. Because of the paucity of contemporary medical facilities, the effectiveness of traditional medicines, and cultural interests and preferences, natural resources provide a low-cost solution for primary care in developing countries [11,12]. A specific physiological response produced by the chemical substances present within the plant is somehow responsible for its medicinal effects on the human body [13]. Therefore, to establish an effective and new drug entity, evaluation of medicinal plants with probable biological activities is irrefutable [14,15].

Oxidative stress is closely related to excessive oxidation, which causes the body to produce a lot of reactive oxygen species (ROS) [16]. Numerous chronic diseases, including cancerous tumors, diabetes, immune system issues, inflammatory joint conditions, cardiovascular and neurological disorders, as well as malignant tumors, are worsened by oxidative stress, which dominated all other global causes of death [17,18]. It has been observed that phytocompounds significantly reduce ROS production and maintain redox homeostasis to prevent oxidative stress [19–21]. Besides, atherosclerosis, thrombosis, plaque rupture, myocardial damage, and failure like major cardiac disorders result from chronic inflammation triggered by oxidative stress [22,23]. According to several epidemiological studies, some inflammatory mediators promote malignant cell proliferation in the tumor microenvironment, induce metastasis and angiogenesis, and reshape the responses to hormones, chemotherapeutic agents, and the body's adaptive immune system [24]. Since oxidative stress and inflammation go hand in hand, it stands to reason that compounds with an antioxidant function would be promising therapeutic options for treating inflammation [25]. Anti-inflammatory action is particularly noteworthy in this study because inflammation is a crucial factor in all chronic diseases. There is mounting evidence that chronic and excessive inflammation plays a significant role in the physiopathology of stress-related diseases, which account for 75–90% of all human illness [26]. As a result, researchers are working to identify and characterize antioxidant phytochemicals or natural treatments to tackle oxidative stress.

Moreover, using a computational technique, plant-based bioactive compounds can be picked from an online library and screened with many target proteins, saving time and money and validating wet-lab results [27,28]. Thus, drug targets and pharmacological pathways can be more accurately anticipated. In silico approaches allow experimental and molecular biologists to create and validate vast amounts of data without wet labs. In recent years, molecular docking and computer-aided drug discovery (CADD) have become popular ways to create a novel moiety [29]. An efficient molecular docking method can pinpoint 3D protein binding location, ligand posture, and physical and chemical interactions [30].

Ophiorrhiza fasciculata D. Don (Family: Rubiaceae) is a flowering perennial herb or subshrub distributed in Nepal, particularly in Raniban, Balaju, Chalnakhel and Kathmundu, in India, mainly in Soureni, Mirik, Durtlang, and Mizoram. Pharmacological investigations on this plant are very limited. However, the genus *Ophiorriza* has been reported to have a variety of biological activities, including anticancer, antiviral, anti-fungal, and anti-malarial properties. For example, the ethanolic extract isolated from the root, stem, and leaf of *O. mungos* possesses antiviral activity and is very effective against the herpes virus [31]. The whole plant of *O. mungos* and *O. prostrata* are reported to have antioxidant and cytotoxic activity [32,33]. A study reported that the root of *O. mungos* possesses high antioxidant activity compared to other parts like the root, stem, and leaf and is also a potent anticancer plant [34]. Krishnakumar et al. [33] compared the cytotoxic activity of the whole plant extract of *O. mungos* with *O. prostrata*. They found that *O. prostrata* holds high cytotoxic activity than the extract of *O. mungos*. These strong biological activities of *Ophiorrhiza* demonstrated the significance of this plant genus in the pharmaceutical industry for the preparation of various drugs. Previous phytochemical studies of this species also lead to the presence of a bioactive quaternary indole alkaloid ophiorrhizine and a quaternary glucoalkaloid bracteatine [35].

Psychotria silhetensis Hook. f. (Family: Rubiaceae) is a small understorey flowering shrub usually observed in open forests or underneath secondary forests and is widely distributed in India, mainly in Assam, Meghalaya, Arunachal Pradesh, Lakhimpur, Sivasagar, and in Bangladesh [36]. Despite no notable phytochemical investigation, the plant revealed a significant level of analgesic, anti-diarrheal, and CNS depressant activities [37] along with beneficial effects on diabetic hyperlipidemia [38]. Other plants of the same genus showed potential biological properties. For example: *P. longipes* and *P. solitudinum* revealed neurodegenerative activity. Antioxidant and antimutagenic activity were demonstrated by *P. umbellata* and *P. brachyceras*, respectively. Likewise, *P. suterela*, *P. stachyoides* showed positive anti-inflammatory effect in in-vitro studies of the crude extract and the leaves of *P. capitata, P. forsteriana* presented cytotoxic activity. Antibacterial activity of *P. rostrata* against *Escherichia coli* and *Staphylococcus aureus* and the anti-fungal effect of *P. spectabilis* against the filamentous fungi *Cladosporium cladosporioides* were remarkable [39].

According to our searching knowledge, no phytochemical and pharmacological studies on the cytotoxicity, thrombolytic, membrane stabilizing, antioxidant, and antibacterial characteristics of these plants have previously been reported. As a result, this work aimed to investigate the lead phytochemicals from these plants and assess their *in vitro* pharmacological activities, focusing on cytotoxicity, thrombolysis, anti-inflammatory, antioxidant, and antibacterial capabilities. Molecular docking was also employed to predict and support the biological activities of the isolated compounds.

2. Materials and methods

2.1. Plant material

The whole plant of *P. silhetensis* was gathered from Moulovibazar Hill tracts in February 2019. The plant *O. fasciculata* was collected from Sylhet in June 2019. A taxonomist and scientific officer of Bangladesh National Herbarium in Dhaka, Bangladesh, recognized and identified both collected plant samples. A voucher specimen has been officially documented for each plant, with an accession number, and securely stored at the Bangladesh National Herbarium in Dhaka for future reference. The accession number for *P. silhetensis* is DACB 56118 and for *O. fasciculata* is DACB 56119.

2.2. Phytochemical investigation: extraction, fractionation, and isolation

The powdered material of freshly collected, shed dried plant of *O. fasciculata* (760 g) and *P. silhetensis* (864 g) were macerated for 25 days using distilled methanol (2.5 L was used for *O. fasciculata* and 3.0 L was used for *P. silhetensis*) accompanying occasional shaking. Subsequently, the solvent mixture was filtered by passing it through a new cotton plug followed by Whatman filter paper. A Buchi Rotavapor (manufactured by BUCHI Labortechnik AG, Flawil, Switzerland) was employed to acquire the concentrated extract. The Rotavapor was operated at 40 °C while maintaining lower pressure conditions [40].

The modified Kupchan technique [41] was used to partition the crude methanolic extracts to find hexane (PSH), dichloromethane (PSDCM), ethyl acetate (PSE), and aqueous (PSM) soluble fractions of both plants. To achieve this goal, 5 gm of raw extract was mixed with a solution containing 10% methanol in water. This mixture was then separated into four distinct fractions by sequentially using n-hexane, dichloromethane (DCM), ethyl acetate, and distilled water as extracting agents. The processes were done for five times. A total of 25 gm of each plant's extract was used for fractionation. Eventually, all of these fractions of the both plants were evaporated until they became dry.

With fine vacuum liquid chromatography (VLC) grade silica (Keisel gel 60H), the crude *O. fasciculata* extract was analyzed using vacuum liquid chromatographic technique. The vacuum was used to fill the column with high-quality fine silica (known as Kiesel gel 60H) until it reached a height of 6 cm. The elution was commenced with n-hexane, polarity of which was gradually increased by adding more polar solvents like ethyl acetate and methanol. Each time, 10 mL of elute was collected into beakers, which were gradually numbered. Moreover, the n-hexane fraction (PSH) of *P. silhetensis* was subjected to silica gel (kieselgel 60H) column chromatography with different ratio of ethyl acetate in hexane solvent system collecting 6 ml of elute at once. The resulting TLC chromatogram was visually examined using UV light at wavelengths of 254 nm and 366 nm to identify any fluorescence quenching effects. Subsequently, the plate was meticulously observed after being treated with a 1% vanillin-sulfuric acid spray. To reveal the presence of colored compounds, the plate was heated at 105 °C for 2–3 min. Finally, ^{1}H NMR spectra of the isolated compounds were captured using a Bruker AMX-400 NMR spectrometer operating at 400 MHz, while the ^{13}C NMR spectra were taken at 100 MHz. All the spectra were gathered in a deuterated solvent ($CDCl_3$), and the chemical shift (δ) values were calibrated against tetramethylsilane (TMS) and the signals from the leftover solvent [42,43].

2.3. Evaluation of cytotoxicity

The bioassay of brine shrimp lethality [44] method has been utilized to assess the cytotoxic effect of the extracts and the fractions. Vincristine sulfate was used as a positive control, and the solvent control dimethyl sulfoxide (DMSO) as a negative control in the experiment [45]. For this experiment, a serial dilution technique was utilized to dissolve 4 mg of each test sample in DMSO, which resulted in variable concentrations (400, 200, 100, 50, 25, 12.5, 6.25, 3.125, 1.5625 and 0.78125 μg/mL) of solution. Ten living nauplii (*Artemia salina*) were placed in each test tube for the experiment and incubated for 24 h at room temperature and in light. The number of living nauplii in each vial was calculated and noted after incubation using a magnifying lens. The following equation (1) was used to determine the nauplii death rate.

$$\% \text{ of mortality} = \text{Number of the nauplii death/number of nauplii taken} \times 100 \ldots \ldots \ldots \quad (1)$$

2.4. Thrombolytic activity

In vitro thrombolytic activity was measured by blood clot lysis method, using a 15,00,000 IU vial of lyophilized streptokinase as a positive control and distilled water as a negative control [46]. Healthy participants' venous blood was collected and incubated for 45 min at 37 °C in pre-weighed sterile microcentrifuge tubes (1 mL/tube). Following the complete extraction of the serum after clot

formation, the clot developed in each tube was weighed. Each microcentrifuge tube containing pre-weighted clot received a separate aqueous solution of 100 μL of different partitions along with crude extract, which was then incubated for 90 min at 37 °C to analyze any clot lyses. The fraction of clot lyses was calculated using the following equation (2):

$$\text{Percent (\%) of clot lysis} = (\text{Released clot weight/clot weight}) \times 100 \ldots \ldots \ldots \quad (2)$$

2.5. Anti-inflammatory effects

Crude methanolic extracts of the plants and the derived fractions were tested for anti-inflammatory effectiveness using two different methods: heat-induced membrane stabilization and hypotonicity-induced HRBC membrane stabilization. Membrane stabilizing behavior in hypotonic and heat-induced solutions has been observed through methods known to utilize the capacity of the Shimadzu UV spectrophotometer at 540 nm to obtain the absorbance values of the supernatant fluids [47].

2.5.1. Hypotonic solution-induced hemolysis

Distinct centrifuge tubes were filled with acetylsalicylic acid (0.10 mg/mL) which is utilized as a standard drug. The tubes were filled with 5 mL of 10 mM sodium phosphate buffer solution (pH 7.4) and 50 mM NaCl (a hypotonic solution) along with 0.50 mL suspension of erythrocyte (RBC) which were incubated at room temperature for 10 min with subsequent centrifugation with an rpm of 3000 for approximately 10 min. After decantation and filtration of the soluble supernatant, the absorbance was measured for each tube. The following equation (3) was used to estimate the stabilization of the membrane:

$$\text{Percent (\%) inhibition of hemolysis} = [(OD_1 - OD_2)/ OD_1] \times 100 \ldots \ldots \ldots \quad (3)$$

OD_1 = Optical density of hypotonic-buffered saline solution (control)
OD_2 = Optical density of test sample in hypotonic solution.

2.5.2. Heat-induced hemolysis

Two separate groups of centrifugation tubes were filled with an extract/fraction of 1 mg/mL together with a 30 μL suspension of erythrocyte and 5 mL of isotonic buffer. The same mixture was used to fill two other centrifugation tubes, except for crude extract/fraction. After gentle inversion of the tubes, one set of tubes was incubated in a water bath at 54°C for 20 min, while the second set was maintained in an ice bath at 0–5°C. To determine the absorbance of the supernatants, centrifugation of the resultant concoction was performed at an rpm of 1300 for 3 min. With the following equation (4), the percent (%) inhibition was calculated:

$$\text{Percent (\%) inhibition of hemolysis} = [\{1 - (OD_2 - OD_1)\}/ (OD_3 - OD_1)] \times 100 \ldots \ldots \ldots \quad (4)$$

OD_1 = unheated test sample, OD_2 = heated test sample and OD_3 = heated control sample.

2.6. Antioxidant activity

The antioxidant activities of the extracts are assessed by DPPH free radical scavenging method, utilizing Tertbutyl-1-hydroxytoluene (BHT) as the positive control [48]. Here, methanolic solution of the extractives and control (2 mL) was interfused with 3.0 mL of a methanolic DPPH solution (20 μg/mL) to obtain several concentrations (500, 250, 125, 62.5, 31.25, 15.625, 7.813, 3.906, 1.953 and 0.977 μg/mL). After a reaction time of about 30 min in dark, the absorbance was determined with methanol as blank at 517 nm with the help of a UV–visible spectrophotometer-1240 (Shimadzu Japan) at 25 °C. Standard and extractives of different concentrations were prepared from mother solutions (1000 μg/mL) by serial dilution technique. The DPPH Free radical inhibition by the samples was measured as a percentage (I%) inhibition with the following equation (5).

$$\text{Percent (I\%) inhibition} = (1 - A_{sample}/A_{blank}) \times 100 \ldots \ldots \ldots \quad (5)$$

A_{blank} = absorbance of the control (with all reagents without the test material). A_{sample} = absorbance of the sample. The IC_{50} value was estimated from the percentage of inhibition plotted against the concentration of the extract.

2.7. Anti-bacterial activity

A total of 13 different types of microbial species, comprising 5 Gram-positive (*Bacillus cereus*, *B. megaterium*, *B. subtilis*, *Staphylococcus aureus* and *Sarcina lutea*) and 8 Gram-negative (*Escherichia coli*, *Pseudomonas aeruginosa*, *Salmonella paratyphi*, *Salmonella typhi*, *Shigella boydii*, *Sh. Dysenteriae*, *Vibrio mimicus* and *V. parahemolyticus*) bacteria, were collected in their pure culture forms from the Bangladesh Council of Scientific and Industrial Research (BCSIR) situated in Dhaka, Bangladesh. The antibacterial activity of the crude plant extracts and their different fractions were evaluated by disc diffusion method [49]. In this process, filter paper discs of 6 mm diameter containing known quantities of test samples were mounted on nutrient agar medium and were seeded with the microorganisms uniformly which later subjected to drying and sterilization. Diffusion of antibiotics occurred through the agar gel from a confined source and generated a gradient of the concentration. Standard antibiotic discs of ciprofloxacin were used as positive control and for negative control blank discs were utilized. These petri dishes were held at low temperature (4 °C) for about 16–24 h to permit

optimum diffusion of the test sample to adjacent media [49] following inversion and incubation at 37 °C for optimum growth of the species for 24 h. Growth of microbes in the media around the discs was halted by the test samples having antibacterial effect and thus yielded a large and distinct place called zone of inhibition whose diameter was then determined to assess antibacterial activity of the test samples [49,50].

2.8. Molecular docking

A computational modeling investigation of these compounds and the chosen reference drugs against their target proteins was conducted to forecast the receptor binding profile of these isolated compounds and support the biological activities of the explored extracts and fractions. Following the procedures outlined in several prior published literatures, the molecular docking intervention of these phytocompounds was performed using PyRx, PyMoL 2.3, and BIOVA Discovery Studio version 4.5 [28,51–55].

2.8.1. Ligand preparation

The structural representation of both separated phytocompounds (**1** and **2**) is shown in Fig. 1. These chemicals were identified as licarin B (PubChem CID: 6441061) and stigmasterol (PubChem CID: 5280794) in the PubChem database (https://pubchem.ncbi.nlm.nih.gov/; retrieved on June 1, 2022).. The standard drugs vincristine (PubChem CID: 5978), warfarin (PubChem CID: 54678486), diclofenac (PubChem CID: 3033), antioxidant BHT (PubChem CID: 31404), and antibacterial agent ciprofloxacin (PubChem CID: 2764) were obtained and secured in SDF format. After serially loading the ligands into Discovery Studio version 4.5, a ligand library in PDB format was constructed utilizing the PubChem CIDs of the ligands. To improve the precision of molecular interaction for all phytoconstituents and standard ligands, the Pm6 semi-empirical technique was applied [56].

2.8.2. Protein preparation

The potential cytotoxicity, thrombolytic, anti-inflammatory, antioxidant, and antibacterial properties of the isolated and identified compounds were projected using computational docking approach. Based on previously published data, the succeeding proteins were chosen for the molecular interaction: epidermal growth factor receptor (PDB ID: 1XKK), tissue plasminogen activator (PDB ID: 1A5H), vFLIP-IKK gamma stapled peptide dimer (PDB ID: 5LDE), glutathione reductase (PDB ID: 3GRS), and dihydrofolate reductase (DHFR) enzyme (PDB ID: 4M6J) to estimate cytotoxicity, thrombolytic, anti-inflammatory, antioxidant, and antibacterial effects, respectively [54,57]. The selected proteins' three-dimensional (3D) crystal structures were obtained from the RCSB protein data bank (https://www.rcsb.org; retrieved on June 1, 2022) and then downloaded in PDB format. All macromolecules were processed with the PyMoL 2.3 tool to remove any water molecules and unneeded protein residues. Non-polar hydrogen atoms were inserted into the cleaned proteins to assemble them. They were then altered to their lowest energy state using a Swiss PDB viewer, an energy minimization tool [58]. After cleaning and optimizing the macromolecules, they were saved in PDB format for further investigation.

2.8.3. Ligand-protein interaction

Utilizing molecular docking, it was inferred the separated plant metabolites' likely binding patterns and affinities for the target biomolecules [59]. A semiflexible modeling approach was used throughout the computationally assisted interaction procedure, which was carried out using the widely used advanced program PyRx AutoDock Vina for molecular docking. The targeted protein had been loaded and assigned a macromolecule label in PyRx. The amino acids with three-letter IDs from the literature [54,57] were chosen to pinpoint the site-specific ligand-protein interaction. All ligands' 3D conformers (in SDF format) were imported into the PyRx program and optimized for energy reduction. All ligands were converted to pdbqt format in the PyRx AutoDock Vina software using the Open Babel tool before the most optimal hit was included. The grid box was then constructed, the active binding sites for the proteins were preserved in its center, and the grid box mapping was documented. The grid box mapping for the 1XKK protein was set to the coordinates: center (X, Y, Z): (16.0758, 34.4556, 35.7611), and dimensions (angstrom) (X, Y, Z): (24.2073, 19.3553, 31.9913). The center grid box mapping for the 1A5H protein was (X, Y, Z): (8.4907, 40.8182, 55.1729), and for the mapping was (X, Y, Z): (19.1990, 24.7990, 20.9212) for dimensions. The center coordinates and dimensions (angstrom) for the 5LDE protein were (X, Y, Z): (−12.3695,

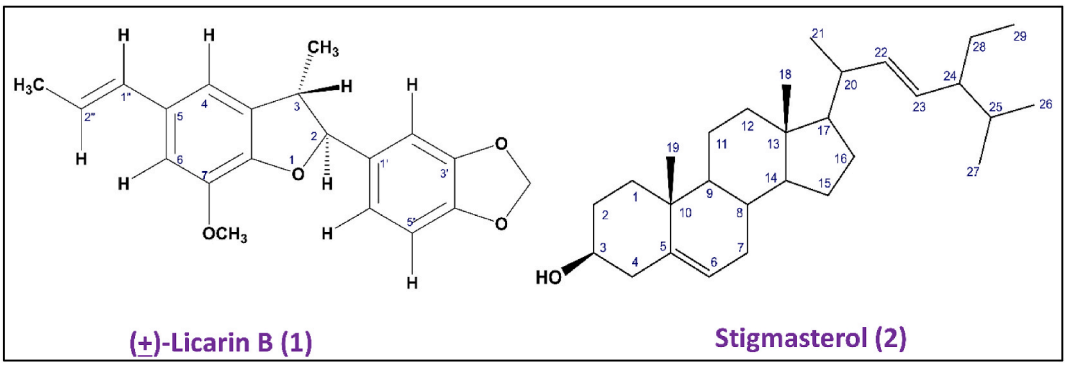

Fig. 1. The chemical structures of the isolated compounds (compound **1**: (±)-Licarin B and compound 2: stigmasterol).

9.9898, −23.5979) and (X, Y, Z): (25.0, 23.1405, 25.0), respectively. Similarly, the center of the generated grid box during the docking with 3GRS protein was (X, Y, Z): (50.4368, 48.1950, 12.3615), and the size was (X, Y, Z): (37.0910, 28.8059, 45.1400). Finally, the center (X, Y, Z): 2.9689, −3.2318, −17.7148) and size (X, Y, Z): 21.7239, 28.4107, 26.8499) of the grid box were recorded during the docking of the compounds with the 4M6J protein. The other docking process parameters were left at their default settings. In all relevant instances, AutoDock Vina was utilized for docking (version 1.1.2). The results of the docking analysis were projected, and the docked macromolecules and ligands were exported as out files (pdbqt format). The out files for the ligands and the pdbqt file for the macromolecule were concatenated and saved in PDB format for further viewing using PyMol software. Then, 3D and 2D figures were visualized and generated using the Discovery Studio Visualizer (version 4.5).

2.9. ADMET and drug-likeliness prediction

The pharmacokinetic properties in terms of absorption, distribution, metabolism, and excretion (ADME) and toxicity were predicted by utilizing the online tool pkCSM (https://biosig.lab.uq.edu.au/pkcsm/prediction; accessed on November 1, 2022). All compounds were evaluated for their potential drug-like qualities using Lipinski's rule of five (molecular weight not exceeding 500; H-bond donors < 5; H-bond acceptors < 10; lipophilicity value LogP ≤ 5; and molar refractivity ranging from 40 to 130) by using the Swiss ADME online tool (www.swissadme.ch; accessed on November 1, 2022).

2.10. Statistical analysis

All *in vitro* analyses were performed using MS Excel version 10.

3. Results

3.1. Phytochemical studies

During the extraction process, 48.9 g of gummy exudate was obtained from *O. fasciculata*, representing a yield of 6.43%. Similarly, *P. silhetensis* yielded 94.5 g of gummy exudate, accounting for 10.93% of the yield. In case of the isolation of phytoconstituents from *O. fasciculata*, the collected elute from beakers 8–9 and 10–11 were mixed and subjected to TLC analysis followed by preparative TLC using 2% ethyl acetate in toluene as a solvent system which led to the isolation of compound **1**. The compound **1** was characterized as (±)-Licarin B (Fig. 1). Furthermore, elute 46–60 (17.5% ethyl acetate in hexane) after TLC monitoring and repetitive preparative TLC revealed the presence of stigmasterol (Fig. 1). Moreover, the purity of the isolated substances was verified by detecting a solitary mark on the TLC plate. The application of vanillin-sulfuric acid spray onto the TLC plate resulted in a pinkish-brown mark, which appeared after a brief heating period, accompanied by calculating R_f value of 0.63 for compound **1**. This was achieved using a solvent system of 5% ethyl acetate in toluene on silica gel PF_{254} plates. In case of compound **2**, when the TLC plate was treated with a solution containing 1% vanillin-sulfuric acid and then subjected to heating at 110 °C for a few minutes, a pink spot emerged. The compound **2** was determined to be soluble in both chloroform and ethyl acetate.

Table 1
^{13}C, ^{1}H, HSQC, DEPT-135, COSY and HMBC spectral data for Compound **1**. [^{13}C: 100 MHz, $CDCl_3$,^{1}H and 2D NMR: 400 MHz, $CDCl_3$].

Position	^{13}C (δ_C, ppm)	^{1}H (δ_H, ppm), J in Hz	HSQC	DEPT-135	COSY	HMBC
2	93.40	5.12 (d, $J = 9.2$)	93.40	CH/CH_3	3.44 (H-3)	106.80 (C-2′); 120.18 (C-6′)
3	45.78	3.44 (m)	45.78	CH/CH_3	5.12 (H-2)	
4	113.38	6.78 (s)	113.38	CH/CH_3		
5	134.38					
6	109.40	6.80 (s)	109.40	CH/CH_3		113.38 (C-4); 134.38 (C-5); 130.94 (C-1″); 144.14 (C-7)
7	144.14					
8	146.54					
9	132.25					
1′	133.11					
2′	106.80	6.95 (s)	106.80	CH/CH_3		147.91 (C-3′); 120.18 (C-6′); 93.40 (C-2)
3′	147.91					
4′	147.61					
5′	108.07	6.80 (d, $J = 8.0$)	108.07	CH/CH_3	6.90 (H-6′)	147.61 (C-4′); 133.11 (C-1′)
6′	120.18	6.90 (d, $J = 15.6$)	120.18	CH/CH_3	6.80 (H-5′)	108.07 (C-5′); 147.61 (C-4′); 93.40 (C-2)
1″	130.94	6.38 (d, $J = 16.0$)	130.94	CH/CH_3	1.89 (2″-CH_3) 6.13 (H-2″)	
2″	123.47	6.13 (dq, $J_d = 16.0$, $J_q = 6.8$)	123.47	CH/CH_3	1.89 (2″-CH_3) 6.38 (H-1″)	
3-CH_3	17.92	1.40 (d, $J = 6.8$ Hz)	17.92	CH/CH_3		45.78 (C-3); 93.40 (C-2)
2″-CH_3	18.34	1.89 (d, $J = 5.6$)	18.34	CH/CH_3	6.13 (H-2″) 6.38 (H-1″)	123.47 (C-2″); 130.94 (C-1″)
7-OCH_3	55.99	3.91 (s)		CH/CH_3		144.14 (C-7)
-CH_2-	101.09	5.98 (s)	101.09	CH_2		147.61 (C-4′); 147.91 (C-3′)

3.1.1. Compound 1 [(±)-Licarin B] from O. fasciculata

Compound **1** was isolated from VLC Fraction No. 4–9 by Preparative TLC of Fraction 8–9 and 10–11 of the methanolic extract of *O. fasciculata* as colorless liquid (Supplementary Table S1). Vanillin-sulfuric acid spray on the developed plate gave a pinkish brown spot after heating for few minutes with R_f value of 0.63 in 5% ethyl acetate in toluene over silica gel PF_{254} plates. The structure of compound **1** was elucidated by extensive NMR studies, including ^{1}H NMR and ^{13}C NMR spectroscopy, DEPT-135, HSQC, HMBC and COSY (Table 1 and supplementary Figures S1-S6). The HMBC and COSY correlation of (±)-Licarin B was showed in Fig. 2.

The ^{1}H NMR signals at δ_H 5.12 (1H, d, $J = 9.2$ Hz) and δ_H 3.44 (1H, m) suggest that the presence of 2, 3-dihydrofuran ring, while the downfield signals at δ_H 6.78 (1H, s) and δ_H 6.80 (1H, s) suggest that the presence of *meta*-disubstituted aromatic ring fused with furan. The ^{13}C NMR signals at δ_C 93.40 (d, C-1), 45.78 (d, C-2), 132.25 (s, C-9), 113.38 (d, C-4), 134.38 (d, C - 5), 109.40 (d, C- 6), 144.14 (s, C-7) and 146.54 (s, C- 8) substantiate the presence of benzofused- 2,3- dihydrofuran ring with the substitution at C-5 and C-7. The additional downfield ^{1}H NMR signals at δ_H 5.98 (2H,s), 6.95 (1H, s), 6.90 (1H,d, $J = 15.6$ Hz) and 6.80 (1H, d, $J = 8.0$ Hz) along with ^{13}C NMR signals at δ_C 101.09 (t, –CH_2-), 106.80 (d, C-2′), 120.18 (d, C-6′), 133.11 (s, C-1′), 108.07 (s, C-5′), 147.61 (s, C-4′) and 147.91 (s, C-3′) confirm the presence of monosubstituted piperonyl moiety. The connectivity of H-2 (δ_H 5.12) with C-2' (δ_C 106.80) and C-6' (δ_C 120.18) in HMQC and the presence of tertiary carbon at C-1′ confirms that the piperonyl moiety is connected to 2, 3-dihydrobenzofuran ring through C-2 and C-1′ linkage. The ^{1}H NMR signal at δ_H 3.91with three proton intensity and ^{13}C NMR signals at δ_C 55.99 (q) is due to the existence of a methoxy groups in the molecule. The ^{1}H NMR signals at δ_H 1.89 (3H, d, $J = 5.6$ Hz), 6.13 (1H, dq, $J_d = 16.0$ Hz, $J_q = 6.8$ Hz) and 6.38 (1H, d, $J = 16.0$ Hz) along with ^{13}C NMR signals at δ_C 18.34(q), 123.47 (d) and 130.94 (d) indicate the presence of propenyl moiety. The singlet carbon signal at C-7 (s, δ_C 144.14) proposes the position of a methoxy group, which leave C-5 position for propenyl moiety. The very up-field doublet at δ_H1.40 in ^{1}H NMR and δ_C 17.92 in CMR suggest the presence of a methyl group at C-3 showed connectivity with C-3 and C-2 in HMBC. Thus, the structure of compound **1** can be proposed as (±)-Licarin B [42]. This is the first report of isolation of this compound from this plant family as of our searching knowledge.

3.1.2. Compound 2 [stigmasterol] from P. silhetensis

During extraction of compound **2**, the used solvent systems as mobile phases in silica gel column chromatography of n-hexane soluble partitionate of *P. silhetensis* are summarized in Supplementary Table S2. Compound **2** showed indications suggestive of a steroidal compound in ^{1}H NMR (400 MHz, $CDCl_3$). It had a one proton multiplet at 3.55, which was at the position and multiplicity of H-3 of a steroidal nucleus. The steroidal skeleton's characteristic olefinic H-6 was seen as a doublet ($J = 7.0$ Hz) at 5.37 that integrated for one proton. At 5.18 and 5.04, it also revealed olefinic protons (H-22 and H-23). Signals at 0.7 and 1.1 (3H each) in the spectrum were assigned to two tertiary methyl groups at C-13 (H_3-18) and C-10 (H_3-19), respectively (Table 2).

The methyl groups at C-25 are responsible for two doublets ($J = 7.0$ Hz) centered at 0.85(H_3-26) and 0.86(H_3-27). The methyl group at C-20 was assigned to the doublets ($J = 6.4$ Hz) at 1.02(H_3-21). The primary methyl linked to C-28, on the other hand, might be attributed to the doublet ($J = 7.0$ Hz) of three proton intensities at 0.92 (H_3-29). The primary methyl group connected to C-18 and C-19 might be attributed to two singlets of three proton intensity at 0.7 and 1.1, respectively (Table 2). The spectrum obtained from ^{1}H NMR has been reported in the supplementary Figure S7. The spectral characteristics described above are quite like those seen in stigmasterol [43]. The identification of Compound **2** was established by co-TLC of the compound with previously identified authentic stigmasterol.

3.2. Cytotoxicity

In a brine shrimp lethality test, the petroleum ether soluble fraction of *O. fasciculata* and the aqueous soluble fraction of *P. silhetensis* showed the highest cytotoxicity ($LC_{50} = 1.41$ g/mL and 1.94 g/mL, respectively) in compared to the standard vincristine sulfate ($LC_{50} = 0.451$ g/mL) (Table 3). Furthermore, both the DCM soluble fraction of *O. fasciculata* and the petroleum ether soluble fraction of *P. silhetensis* ($LC_{50} = 12.13$ g/mL and 8.71 g/mL, respectively) exhibited mild lethality whereas the remaining fractions of both plants revealed poor cytotoxicity (Table 3). It is noted that the detailed calculation with the curves have been tabulated in Supplementary Tables S3–S12.

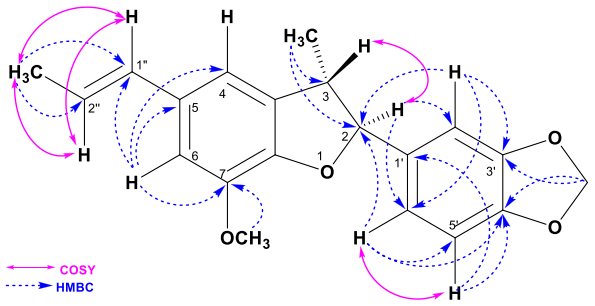

Fig. 2. HMBC and COSY correlation of (±)-Licarin B.

Table 2
^{1}H NMR spectral data of Compound **1** and the reference values of ^{1}H NMR obtained from Chaturvedula et al. [43], in $CDCl_3$.

Position	Compound 1	Stigmasterol [43]
	δ_H, multi, *J* in Hz	δ_H, multi, *J* in Hz
H-3	3.55, m	3.52, m
H-6	5.37, d (*J* = 7.0 Hz)	5.35, d (*J* = 7.0 Hz)
H_3-18	0.7, s	0.69, s
H_3-19	1.1, s	1.01, s
H_3-21	1.02, d (*J* = 6.4 Hz)	1.02, d (*J* = 6.6 Hz)
H-22	5.18, dd (*J* = 12 and 8 Hz)	5.15, dd (*J* = 12 and 8 Hz)
H-23	5.04, dd (*J* = 12 and 8 Hz)	5.03, dd (*J* = 12 and 8 Hz)
H_3-26	0.84, d (*J* = 7.0 Hz)	0.79, d (*J* = 7.0 Hz)
H_3-27	0.80, d (*J* = 7.0 Hz)	0.84, d (*J* = 7.0 Hz)
H_3-29	0.92, d (*J* = 7.0 Hz)	0.80, d (*J* = 7.0 Hz)

Table 3
In vitro cytotoxic properties with LC_{50} (obtained from brine shrimp lethality assay) values of methanolic extracts and their various solvent fractions of *Ophiorrhiza fasciculata* and *Psychotria silhetensis*.

Test samples	*Ophiorrhiza fasciculata*	*Psychotria silhetensis*
	LC_{50} (μg/mL)	LC_{50} (μg/mL)
Methanol (crude) extract	31.08	26.23
Petroleum ether fraction	1.41	8.71
Dichloromethane fraction	12.13	164.55
Chloroform fraction	51.27	215.54
Aqueous fraction	174.4	1.94
Vincristine sulfate (Standard)	0.451	0.451

3.3. Thrombolytic activity

The crude methanolic extracts and different soluble fractions of both *P. silhetensis* and *O. fasciculata* were assessed for thrombolytic activity using streptokinase as a positive control and distilled water as a negative control. The petroleum ether soluble fraction of *O. fasciculata* and the aqueous soluble fraction of *P. silhetensis* had the highest thrombolytic activity (*in vitro*), with 46.66% and 50.10% clot lyses, respectively (Table 4).

3.4. Anti-inflammatory

In hypotonic and heat-induced conditions, the crude extract and dichloromethane soluble fraction of *O. fasciculata* prevented human erythrocyte hemolysis by 64.03% and 37.08% respectively, compared to the value of 81.97% and 42.12% shown by acetyl salicylic acid (standard drug) (Table 3). Likewise, in conditions affected by hypotonic solution and heat, the aqueous fraction of *P. silhetensis* reduced human erythrocyte hemolysis by 17.59% and 32.47%, respectively, compared to 72.30% and 41.9% for the same standard acetylsalicylic acid (Table 5). It is noted that the detailed calculation has been tabulated in Supplementary Tables S13–S16.

3.5. Antioxidant

The antioxidant activity of different extractives was compared to that of conventional BHT in the study (Table 4). When compared to BHT (IC_{50} = 21.20 μg/mL), the aqueous soluble fraction, chloroform fraction, and petroleum ether fraction of *O. fasciculata* had the

Table 4
In vitro thrombolytic properties with % lysis of methanolic extracts and their various solvent fractions of *Ophiorrhiza fasciculata* and *Psychotria silhetensis*.

Test samples	*Ophiorrhiza fasciculata*	*Psychotria silhetensis*
	% clot lyses	% clot lyses
Methanol extract	10.93	16.59
Petroleum ether fraction	46.66	6.32
Dichloromethane fraction	30.26	23.74
Chloroform fraction	24.72	8.34
Aqueous fraction	11.64	50.10
Blank	5.44	5.44
Streptokinase	66.98	66.98

Table 5
Anti-inflammatory effects (% inhibition of hemolysis) of methanolic extracts and their various solvent fractions of *Ophiorrhiza fasciculata* and *Psychotria silhetensis*.

Test samples	*Ophiorrhiza fasciculata*		*Psychotria silhetensis*	
	% Inhibition of hemolysis		% Inhibition of hemolysis	
	Hypotonic solution-induced	Heat-induced	Hypotonic solution-induced	Heat-induced
Methanol extract	64.03	31.20	5.99	2.02
Petroleum ether fraction	63.94	34.97	5.08	20.62
Dichloromethane fraction	38.76	37.08	12.96	10.70
Chloroform fraction	29.34	28.68	7.20	24.19
Aqueous fraction	23.84	11.03	17.59	32.47
Acetylsalicylic acid	81.97	42.12	72.30	41.90

promising antioxidant activity (IC_{50} = 7.22, 26.88, and 79.39 μg/mL, respectively), whereas all other fractions of both plant had a negligible scavenging effect (Table 6).

3.6. Antibacterial effects

For anti-bacterial screening, chloroform, and dichloromethane soluble fraction of *P. silhetensis* showed a minute activity against bacterial growth whereas no extracts or fractions of *O. fasciculata* exhibited any antibacterial activity when compared to standard ciprofloxacin (Table 7).

3.7. Molecular docking

In order to understand the mechanism of pharmacological activities of the extracts and fractions obtained from *O. fasciculata* and *P. silhetensis*, molecular docking of the plant-derived bioactive components to the corresponding molecular receptors was performed using numerous applicable computer-based approaches. The results of PyRx docking are all shown in Table 8 and Fig. 3 (A-J) and 4 (A-J). The amino acids that interact with the ligand atoms are listed in Supplementary Tables S17 and S18, together with information about the interactions' nature, bond types, and bond lengths. The binding strength increases as the binding affinity's numerical value (kcal/mol) decreases. The best docking prediction was the anticipated binding affinity, which had a zero root mean square deviation [44]. Both isolated compounds **1** and **2** (licarin B and stigmasterol) exerted higher binding affinities towards the epidermal growth factor receptor (−9.5 and −9.8 kcal/mol), tissue plasminogen activator (−7.9 and −7.7 kcal/mol), vFLIP-IKK gamma stapled peptide dimer (−6.3 and 7.0 kcal/mol), glutathione reductase (both are −8.5 kcal/mol), and dihydrofolate reductase enzyme (both are −8.4 kcal/mol),revealing better cytotoxic, thrombolysis, anti-inflammatic, antioxidative, and antibacterial potentials than the standard drugs vincristine, warfarin, diclofenac, butylated hydroxytoluene, and ciprofloxacin. Fig. 3 (A-J) displays the 3D and 2D molecular interactions of compound **1** (licarin B) with these chosen proteins. Similarly, Fig. 4 (A-J) depicts the 3D and 2D molecular interactions of compound **2** (stigmasterol) with these specific proteins.

3.8. ADMET prediction and drug-likeliness

Poor absorption, distribution, metabolism, excretion, and toxicological profiles are widely acknowledged to hinder effective pharmacological action. The biggest downside of drug development in clinical research is its pharmacokinetic features, which may make it exceedingly pricey. Consequently, *in silico* techniques were utilized to evaluate ADMET properties and estimate the drug likeliness of the isolated compounds being therapeutic development candidates [60–62]. All the values obtained from the server-based ADMET and drug likeness analyses were tabulated in Table 9. Notably, both isolated compounds showed high intestinal absorption rate (licarin B = 96.57% and stigmasterol = 94.97%) and good Caco2 permeability. Both compounds acted as P-glycoprotein I inhibitors and showed good volume of distribution at steady state (VDss). Compound **2** exerted the higher blood-brain barrier (BBB) permeability than the compound **1**.

Table 6
Antioxidant potentials with IC_{50} (obtained from DPPH assay) of methanolic extracts and their various solvent fractions of *Ophiorrhiza fasciculata* and *Psychotria silhetensis*.

Test samples	*Ophiorrhiza fasciculata*	*Psychotria silhetensis*
	IC_{50} (μg/mL)	IC_{50} (μg/mL)
Methanol (crude) extract	822.7	573.07
Petroleum ether fraction	79.39	1294.38
Dichloromethane fraction	742.62	370.09
Chloroform fraction	26.88	239.85
Aqueous fraction	7.22	341.77
BHT	21.20	21.20

Table 7
Antibacterial effects of dichloromethane and chloroform fractions of *Psychotria silhetensis*.

Test Organism	*P. silhetensis* (zone of inhibition, mm)		Standard drug (ciprofloxacin)
	Dichloromethane fraction	Chloroform fraction	
Bacillus cereus	8	8	40
Bacillus megaterium	8	10	42
Bacillus subtilis	0	8	38
Staphylococcus aureus	0	8	41
Sarcina lutea	8	12	37
Escherichia coli	0	0	38
Pseudomonas aeruginosa	8	8	45
Salmonella paratyphi	0	0	43
Salmonella typhi	0	8	39
Shigella boydii	10	0	42
Shigella dysenteriae	8	12	40
Vibrio mimicus	8	10	40
Vibrio parahemolyticus	0	0	47

Table 8
Molecular docking scores or binding affinity (kcal/mol) retrieved from *in silico* interactions of the isolated compounds licarin B, stigmasterol, and the standard drugs during the interaction with epidermal growth factor receptor (PDB ID: 1XKK), tissue plasminogen activator (PDB ID: 1A5H), vFLIP-IKK gamma stapled peptide dimer (PDB ID: 5LDE), glutathione reductase (PDB ID: 3GRS), and dihydrofolate reductase (DHFR) enzyme (PDB ID: 4M6J) for assessing the cytotoxicity, thrombolytic, anti-inflammatory, antioxidant, and antibacterial activities, respectively.

Com. No.	Name of Compounds/Drugs	PubChem ID	Binding affinity towards corresponding receptors/macromolecules (kcal/mol)				
			1XKK (Cytotoxicity)	1A5H (Thrombolytic)	5LDE (Anti-inflammatory)	3GRS (Antioxidant)	4M6J (Antibacterial)
1	Licarin B	6441061	**−9.5**	**−7.9**	**−6.3**	**−8.5**	**−8.4**
2	Stigmasterol	5280794	**−9.8**	**−7.7**	**−7.0**	**−8.5**	**−8.4**
Standard drugs	Vincristine	5978	−5.8				
	Warfarin	54678486		−7.4			
	Diclofenac	3033			−5.5		
	BHT	31404				−5.8	
	Ciprofloxacin	2764					−8.2

BHT = Butylated hydroxytoluene.

Inhibiting the human cytochrome (CYP450) and its primary isoforms (CYP2D6 and CYP3A4), which are responsible for liver metabolism, may result in drug toxicity and other side effects, such as drug-drug interactions [61,62]. In our study, no compound acted as CYP2D6 and CYP3A4 inhibitors. In the case of renal clearance, compound **2** (stigmasterol) exhibited total clearance (expressed as log ml/kg/min) 0.618 and acted as renal OCT2 (organic cation transporter 2) non-substrate. Both compounds showed no AMES toxicity and hepatotoxicity. Besides, the compounds have exhibited no association with skin sensitization and no inhibition of hERG I (Table 9). The obtained LD_{50} values of the substances indicated no acute oral toxicity according to the OECD 423 model [63], and they were classified as class VI ('non-toxic') according to the Oral Toxicity Classification. Moreover, both drugs satisfied Lipinski's rule of five with a bioavailability score of 0.55 in drug likeliness analysis.

The bioavailability radar images of the isolated compounds have been presented in Fig. 5 (A, B), where the oral bioavailability space is marked by the pink area. The radar profile of a compound must perfectly match it to function as a drug-like moiety. Although the radar profile of compound **1** entirely fitted within the pink area, the compound **2** violated two criteria, i.e., lipophilicity ($-0.7 <$ XLOGP3 $< +5.0$) and insolubility ($0 <$ LogS (ESOL) < 6).

Moreover, two pharmacokinetic features that must be evaluated at various stages of the drug development process are gastrointestinal absorption and blood-brain barrier (BBB) permeability. Using the brain or intestinal estimated permeation (BOILED-Egg) model based on the lipophilicity (WLOGP) and polarity (topological polar surface area (TPSA), these two parameters of the isolated compounds (**1** and **2**) were assessed (Fig. 6). The BOILED-Egg model offers an excellent contribution to lead optimization. In order to estimate the passive gastrointestinal absorption and brain access of small molecules, the model offers a quick, intuitive, easily reproducible, yet statistically unprecedented robust method [64]. The compounds in the white area have high intestine absorption, but the molecules inside the yolk (yellow area) have high BBB permeability (Fig. 6). The color of the dots indicates whether a molecule is a P-glycoprotein substrate (blue) or non-substrate (red) [61]. Accordingly, the compound **1** exerted high penetration to BBB and the compound was found to be P-glycoprotein non-substrate.

4. Discussion

Compounds originating from plants are currently being used to treat a wide range of physiological conditions. In recent years, natural therapies based on medicinal plants and herbs have gained popularity due to their efficiency, purity, and cost-effectiveness in

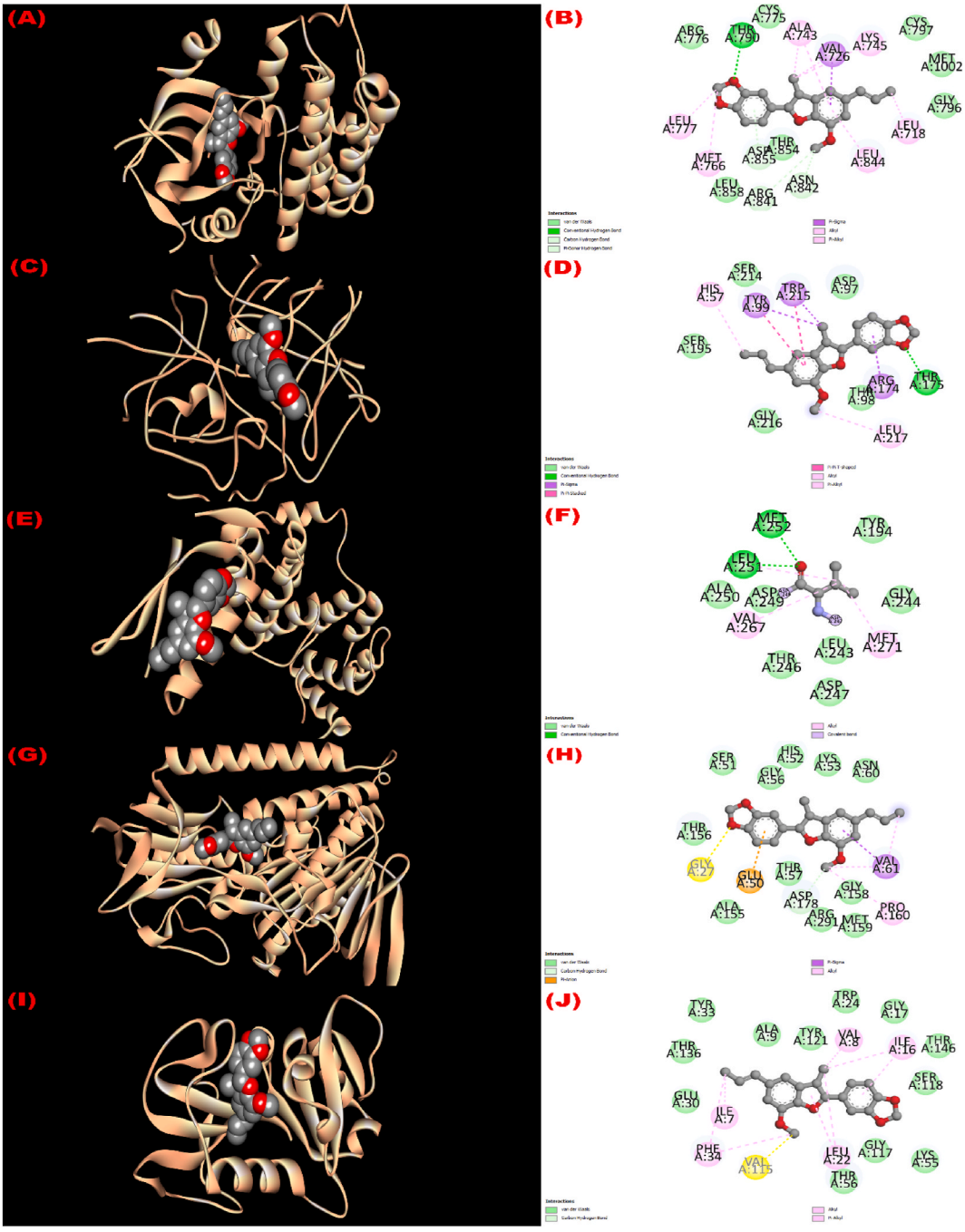

Fig. 3. The 3D and 2D molecular interactions of compound **1** (licarin B) with the epidermal growth factor receptor (PDB ID: 1XKK) (**A,B**), tissue plasminogen activator (PDB ID: 1A5H) (**C,D**), vFLIP-IKK gamma stapled peptide dimer (PDB ID: 5LDE) (**E,F**), glutathione reductase (PDB ID: 3GRS) (**G,H**), and dihydrofolate reductase (DHFR) enzyme (PDB ID: 4M6J) (**I,J**) for assessing the cytotoxicity, thrombolytic, anti-inflammatory, antioxidant, and antibacterial activities, respectively.

treating various diseases [65,66]. The present study has demonstrated the isolation and identification of licarin B and stigmasterol from *O. fasciculata* and *P. silhetensis*, respectively. Based on a thorough literature search, we believe this is the first report of isolating all these constituents (compound **1** and **2**) from these plant species. The current investigation also revealed potential cytotoxic, thrombolytic, anti-inflammatory, antioxidant, and antibacterial activities of the crude extracts and their several solvent fractions derived from the plants.

The present study focused on evaluating different extractives of *O. fasciculata* and *P. silhetensis* for their several bioactivities and

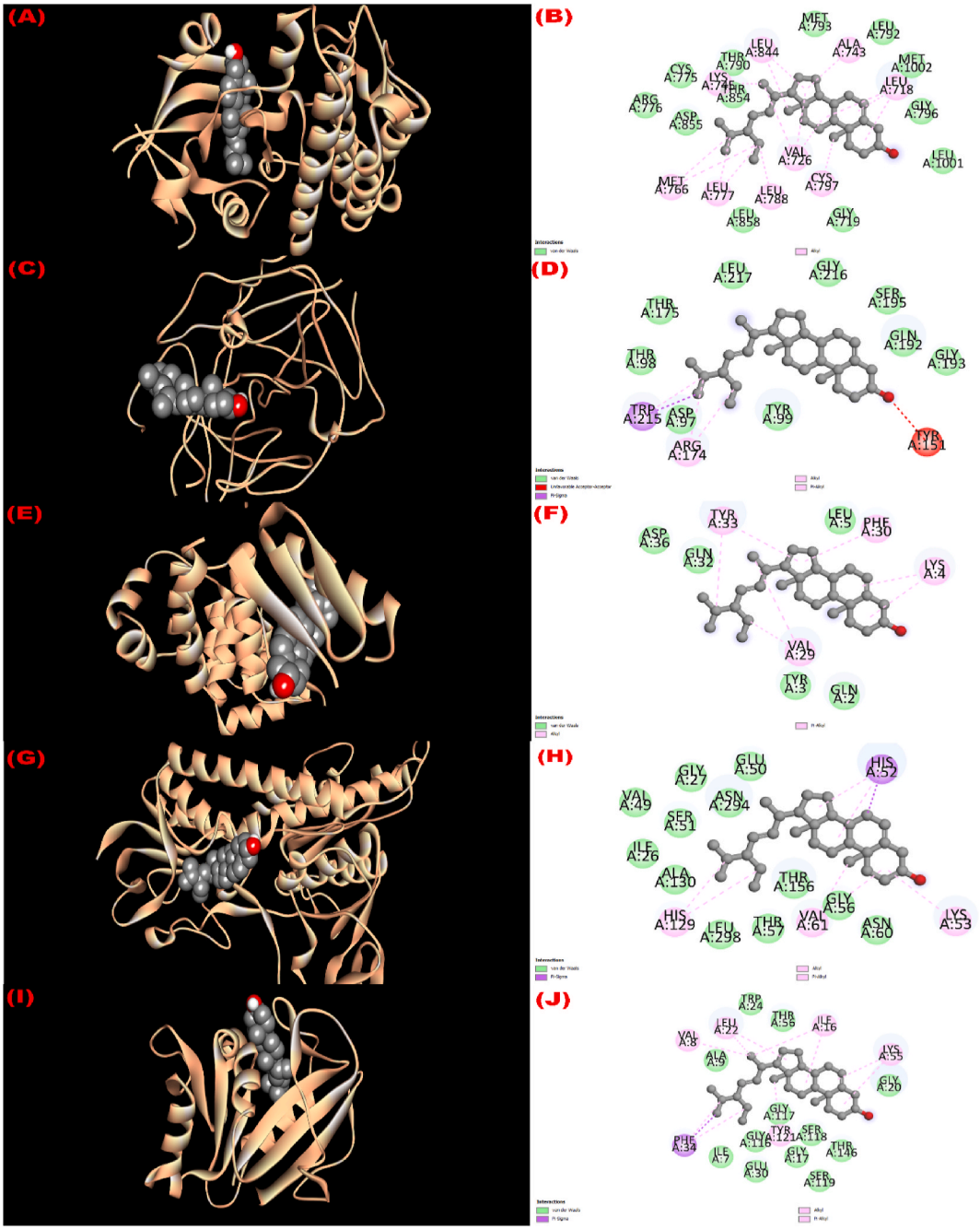

Fig. 4. The 3D and 2D molecular interactions of compound **2** (stigmasterol) with the epidermal growth factor receptor (PDB ID: 1XKK) (**A,B**), tissue plasminogen activator (PDB ID: 1A5H) (**C,D**), vFLIP-IKK gamma stapled peptide dimer (PDB ID: 5LDE) (**E,F**), glutathione reductase (PDB ID: 3GRS) (**G,H**), and dihydrofolate reductase (DHFR) enzyme (PDB ID: 4M6J) (**I,J**) for assessing the cytotoxicity, thrombolytic, anti-inflammatory, antioxidant, and antibacterial activities, respectively.

concluded that the petroleum ether soluble fraction of *O. fasciculata* and aqueous soluble fraction of *P. silhetensis* retained potent cytotoxic characteristics based on LC_{50} values at low concentrations, and therefore needed to be evaluated against cell lines both cancerous and normal. It has been shown that petroleum ether and dichloromethane soluble fractions of *O. fasciculata* exerted higher cytotoxicity, which may contain cytotoxic or anticancer molecules. In addition, the binding affinity (kcal/mol) of the both isolated compounds were significantly higher than that of the standard vincristine when docked against the epidermal growth factor receptor (EGFR) protein. This protein is directly involved in the process of cellular signal transduction as well as the maintenance of cellular functions. Numerous cancer types, including ovarian, breast, and colon cancer, progress more quickly when EGFR is overproduced

Table 9
Absorption, distribution, metabolism, excretion, toxicity (ADMET) and drug-likeliness prediction of the isolated compounds.

Properties	Model name (Unit)	Compounds	
		Licarin B (1)	Stigmasterol (2)
Absorption	Water solubility (log mol/L)	−5.195	−6.682
	Caco2 permeability (log Papp in 10^{-6} cm/s)	2.236	1.213
	Intestinal absorption (human) (% absorbed)	96.573	94.97
	Skin Permeability (log Kp)	−2.496	−2.783
	P-glycoprotein substrate	Yes	No
	P-glycoprotein I inhibitor	Yes	Yes
	P-glycoprotein II inhibitor	No	Yes
Distribution	VDss (human) (log L/kg)	0.502	0.178
	BBB permeability (log BB)	−0.136	0.771
	CNS permeability (log PS)	−1.528	−1.652
Metabolism	CYP2D6 substrate	No	No
	CYP3A4 substrate	Yes	Yes
	CYP2D6 inhibitior	No	No
	CYP3A4 inhibitior	No	No
Excretion	Total Clearance (log ml/min/kg)	0.034	0.618
	Renal OCT2 substrate	Yes	No
Toxicity	AMES toxicity	No	No
	hERG I inhibitor	No	No
	Hepatotoxicity	No	No
	Skin Sensitization	No	No
	Oral Rat Acute Toxicity (LD_{50}) (mol/kg)	2.416	2.54
	Oral Rat Chronic Toxicity (LOAEL) (log mg/kg_bw/day)	1.837	0.872
Drug-likeness	Lipinski's Rule of Five	Yes	Yes
	Bioavailability Score (%)	0.55	0.55

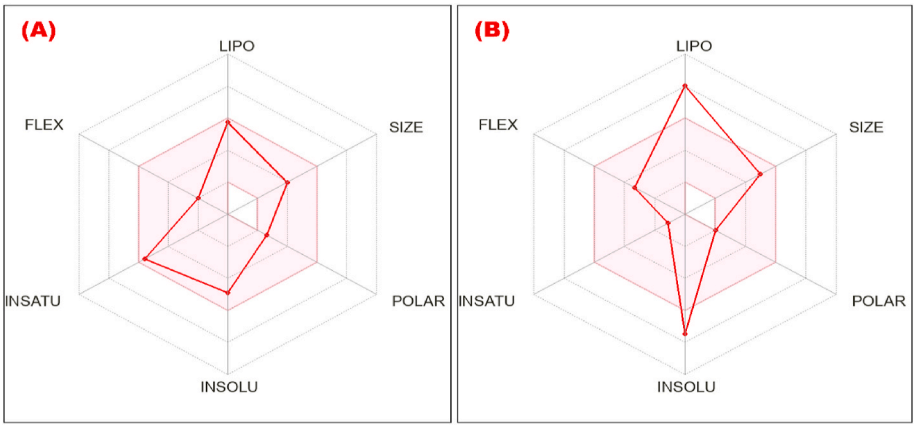

Fig. 5. Physicochemical radar images of the isolated compounds [(A) = licarin B and (B) = stigmasterol)] considering six physicochemical parameters (lipophilicity, size, polarity, solubility, flexibility, and saturation), where the colored zone is suitable for oral bioavailability. [Here; LIPO = Lipophilicity (−0.7 < XLOGP3 < +5.0), SIZE = 150 g/mol < MV < 500 g/mol, POLAR (Polarity) = 20 Å^2 < TPSA <130 Å^2, INSOLU (Insolubility) = 0 < LogS (ESOL) < 6, INSATU (Instauration) = 0.25 < Fraction Csp3 < 1, FLEX (Flexibility): 0 < Num. of rotatable bonds <9].

[54]. The extracellular signal-regulated kinase (ERK) pathway is stimulated by EGFR, whereas the c-Jun NH_2-terminal kinase (JNK) and p38 signaling pathways are activated by ROS, UV radiation, and inflammatory cytokines such as tumor necrosis factor-alpha (TNF-α)- and interleukin (IL)-1 [67]. Therefore, inhibiting EGFR could be an intriguing target for developing particular anticancer agents [54]. The activities could be attributed to the compound's propensity for hydrophobic interactions with proteins via alkyl, pi-alkyl and pi-sigma bonds. Licarin B, compound **1**, demonstrated the formation of three H-bonds. Both substances (compounds **1** and **2**) showed superior fit to the EGFR active sites and generated 9 to 15 hydrophobic contacts. Numerous researches have noted the anti-proliferative effects of licarin B, even though its exact mode of action is yet unknown [68]. Furthermore, stigmasterol (compound **2**) has exerted anti-carcinogenic effects reported in many studies [69–71]. The compound **2** shows anticancer effects in a variety of methods, most notably by drastically decreasing the transcript level of tumor necrosis factor-alpha (TNF-α), activating the ER-mitochondrial axis, and inducing apoptosis caspase-8, 9 [69,72,73].

Thrombosis is one of the leading causes of morbidity and mortality across a broad spectrum of vascular illnesses [74]. In presence of activated thrombin, the conversion of fibrinogen to fibrin results in the formation of a thrombus or blood clot. Damaged tissues release

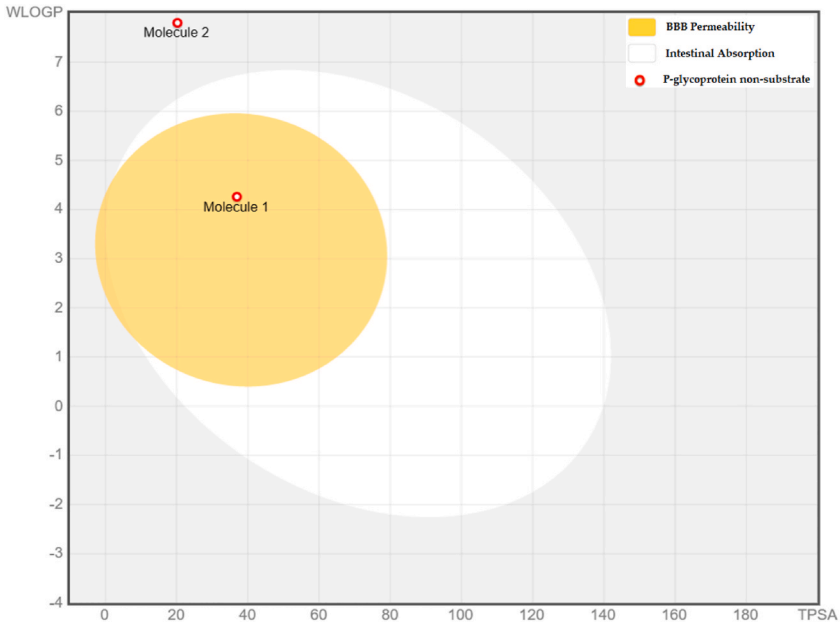

Fig. 6. BOILED-Egg model for predicting blood-brain barrier (BBB) permeability and intestinal absorption of the isolated compounds: (molecule 1) licarin (B) and (molecule 2) stigmasterol. [BBB = Blood-Brain Barrier, HIA = Human Intestinal Absorption, TSPA = topological polar surface area, WLogP = LogP value calculated according to the Wildman–Crippen method].

tissue plasminogen activator (t-PA), which transforms plasma protein plasminogen into plasmin, dissolving the blood clot. Patients with blocked veins or arteries are treated with fibrinolytic medications that eradicate thrombi by activating tissue plasminogen activator (t-PA) and exerting a thrombolytic effect [75]. Reducing platelet aggregation is protective against certain heart disorders, such as atherosclerosis [76]. In this current study, the petroleum ether soluble fraction of *O. fasciculata* and aqueous soluble fraction of *P. silhetensis* exhibited significant thrombolytic activity (46.66% and 50.10% clot lysis, respectively). This finding may benefit the development of recombinant variants of first-generation thrombolytic agents associated with systemic fibrosis and bleeding complications [77,78]. In addition, the binding affinities towards human tissue plasminogen activator of both substances isolated from these plants (licarin B = −7.9 kcal/mol and stigmasterol = −7.7 kcal/mol) were greater than those of the conventional thrombolytic drug warfarin (−7.4 kcal/mol). Although there is no clear evidence that licarin B inhibits platelet aggregation, several other lignans have demonstrated thrombolytic activity in numerous investigations [79].

Drugs capable of stabilizing erythrocyte membrane can also stabilize lysosomal membrane and therefore can exhibit anti-inflammatory properties by altering the activity and release of cell mediators due to the resembles between them [47,80]. Here, the methanol as well as dichloromethane soluble fractions of *O. fasciculata* and aqueous soluble fraction of *P. silhetensis* demonstrated noticeable anti-inflammatory activity by preventing the hemolysis of erythrocytes in conditions stimulated by hypotonic solution and heat. In addition, both isolated drugs have increased binding affinities for the vFLIP-IKK gamma stapled peptide dimer (PDB ID: 5LDE) protein, supporting the *in vitro* study's findings.

When tissues mature, they undergo a variety of oxidative injuries including DNA oxidative stress, oxidative protein injury, lipid peroxidation, and other oxidative ailments [81,82]. So, there is a great deal of concern in the development of plant based natural antioxidant [83] due to harmful and cancerous effects of synthetic antioxidants [84,85]. Here, in our search of new and potential natural antioxidants, we evaluated different extractives of *O. fasciculata* and *P. silhetensis* where aqueous soluble fraction of *O. fasciculata* and chloroform soluble fraction of *P. silhetensis* sustained the maximum antioxidant activity as compared to standard BHT. Notably, the aqueous fraction of *O. fasciculata* exerted promising antioxidant effect with IC_{50} value of 7.22 μg/mL compared to the reference standard drug BHT (IC_{50} = 21.20 μg/mL). Besides, the both isolated compounds displayed higher binding affinities (−8.5 kcal/mol) towards the glutathione reductase enzyme than the standard drug BHT (−5.8 kcal/mol). Any hydrophobic interactions between the compound and the glutathione reductase enzyme via alkyl and pi-alkyl interactions may result in these consequences [54]. The compound **1** (licarin B) has showed antioxidant effect in the study done by Hou et al. [86]. In addition, the antioxidant effects of stigmasterol in various ways have been explained in various studies. Specifically, stigmasterol decreases hepatic lipid peroxidation and enhances the activities of catalase, superoxide dismutase, and glutathione, revealing that it possesses antioxidant capabilities [87,88].

The antibacterial activity of the extracts was evaluated to find new sources of antimicrobial lead compounds. This is because nearly all conventional antibiotics are becoming resistant to multiple strains of bacteria and displaying greater adverse effects than the traditional treatments [89]. Antimicrobial-resistant microorganisms are found to be the cause of approximately 700,000 deaths annually across the globe [90]. Though the current study found no connection of antibacterial activity with any of the extractives of

O. fasciculata, the dichloromethane and chloroform soluble factions of *P. silhetensis* demonstrated antibacterial effect when tested against a series of gram-positive and gram-negative bacteria and therefore pointed towards the way to develop new antibiotic agents from the plant. Inhibition of bacterial cell wall production, suppression of bacterial protein biosynthesis, obstruction of bacterial DNA replication, and inhibition of bacterial folic acid metabolism all may contribute to the antibacterial activity of the extract or its fractions [91]. In addition, the isolated compounds showed interesting binding affinities (−8.4 kcal/mol) towards dihydrofolate reductase (DHFR) enzyme compared to the standard drug ciprofloxacin (−8.2 kcal/mol). According to Mailafiya et al. [92], the isolated stigmasterol is a potent, broad-spectrum antibacterial and antifungal agent that could be employed as a precursor chemical in the development of new antimicrobial medicines. However, the cause of the lack of antibacterial activity of *O. fasciculata* remains unidentified. It may be necessary to do additional research to validate the result and determine its underlying causes.

Moreover, the current study found favorable pharmacokinetics and drug like properties of the isolated compounds with free of oral acute toxicity. As the log scale of water solubility ranges from −4.0 log mol/L to 0 log mol/L [62], the both compounds showed no water solubility. Furthermore, human ether-a-go-go-related gene (hERG) blockage caused by drugs continues to be a significant barrier to developing new and safe therapies. Due to their severe cardiotoxic side effects via off-target interactions with hERG, various drugs have been withdrawn from the market or promising drug candidates have been postponed from further investigations [93,94]. As the isolated compounds showed no inhibition of the hERG I receptor, both drugs may be considered free of cardiotoxicity. With respect to the prediction of human intestinal absorption and brain permeation capability of the isolated compounds, the "BOILED-egg" model of the both compounds were studied based on the Swiss ADME online tool. Compound **1** exerted high BBB permeability due to its low molecular weight (324.37 g/mol), number of rotatable bonds (n = 3), number of hydrogen bond acceptors (n = 4), and TSPA 36.92 $Å^2$ [95].

5. Limitations

Although there are many strong points of the current study, it has some flaws as well. The study did not conduct thorough phytochemical investigations. Besides, the study predicted the pharmacological effects of the isolated compounds via *in-silico* techniques with no experimental validation.

6. Conclusion

The research reports the isolation of a neolignans (±)-Licarin B from *Ophiorrhiza fasciculata* and a triterpene stigmasterol from *Psychotria silhetensis*, which were characterized by extensive spectroscopic methods. The present study concluded that different partitionates of methanolic extracts of the whole plant of *Ophiorrhiza fasciculata* exerted significant thrombolytic, cytotoxic and promising antioxidant activity with IC_{50} value of 7.22 μg/mL (aqueous soluble fraction of *O. fasciculata*). Likewise, different partitions of methanolic extracts of the whole plant of *Psychotria silhetensis* showed significant thrombolytic and cytotoxic activity, with mild antioxidant and antimicrobial effects. Furthermore, because both isolated compounds showed encouraging binding affinities for the corresponding receptors, and thus, the *in-silico* analyses corroborated the *in vitro* results. Based on these findings, it is recommended that further investigation needs to be conducted on these plants to uncover other bioactive chemicals, assess their unknown efficacy, and validate their use as traditional remedies.

Author contribution statement

Parisa Tamannur Rashid; Md. Jamal Hossain: Conceived and designed the experiments; Performed the experiments; Analyzed and interpreted the data; Wrote the paper.

Miss Sharmin Zahan: Performed the experiments; Analyzed and interpreted the data; Wrote the paper.

Choudhury Mahmood Hasan; Mohammad A. Rashid; Muhammad Abdullah Al-Mansur: Analyzed and interpreted the data.

Mohammad Rashedul Haque: Conceived and designed the experiments; Analyzed and interpreted the data.

Data availability statement

Data included in article/supp. material/referenced in article.

Declaration of competing interest

The authors declare that they have no known competing financial interests or personal relationships that could have appeared to influence the work reported in this paper.

Acknowledgement

The authors deeply appreciate the support and co-operation offered by the Department of Pharmaceutical Chemistry, University of Dhaka, and Department of Pharmacy, State University of Bangladesh during the timeline of this study.

Appendix A. Supplementary data

Supplementary data to this article can be found online at https://doi.org/10.1016/j.heliyon.2023.e20100.

References

[1] A.G. Atanasov, S.B. Zotchev, V.M. Dirsch, International natural product sciences taskforce, supuran CT. Natural products in drug discovery: advances and opportunities, Nat. Rev. Drug Discov. 20 (2021) 200–216, https://doi.org/10.1038/s41573-020-00114-z.

[2] D.J. Newman, G.M. Cragg, Natural products as sources of new drugs over the nearly four decades from 01/1981 to 09/2019, J. Nat. Prod. 83 (2020) 770–803, https://doi.org/10.1021/acs.jnatprod.9b01285.

[3] S.A. Baba, M. Vahedi, I. Ahmad, B.S. Rajab, A.O. Babalghith, S. Irfan, M.J. Hossain, *Crocus sativus* L. Tepal extract induces apoptosis in human U87 glioblastoma cells, BioMed Res. Int. 2022 (2022), 4740246, https://doi.org/10.1155/2022/4740246.

[4] L.F. González Arbeláez, A. Ciocci Pardo, J.C. Fantinelli, G.R. Schinella, S.M. Mosca, J.L. Ríos, Cardioprotection and natural polyphenols: an update of clinical and experimental studies, Food Funct. 9 (2018) 6129–6145, https://doi.org/10.1039/c8fo01307a.

[5] B.J. Guo, Z.X. Bian, H.C. Qiu, Y.T. Wang, Y. Wang, Biological and clinical implications of herbal medicine and natural products for the treatment of inflammatory bowel disease, Ann. N. Y. Acad. Sci. 1401 (2017) 37–48, https://doi.org/10.1111/nyas.13414. PMID: 28891095.

[6] A. Roy, C. Pandit, A. Gacem, M.S. Alqahtani, M. Bilal, S. Islam, M.J. Hossain, M. Jameel, Biologically derived gold nanoparticles and their applications, Bioinorgan. Chem. Appl. 2022 (2022), 8184217, https://doi.org/10.1155/2022/8184217.

[7] WHO, Guidelines on registration of traditional medicines in the WHO African Region, in: Brazzaville, World Health Organization Regional Office for Africa, 2004. AFR/TRM/04.1), http://whqlibdoc.who.int/afro/2004/AFR_TRM_04.1.pdf. (Accessed 1 July 2022).

[8] WHO, Traditional Medicines: Global Situation, Issues and Challenges, World Health Organization, Geneva, Switzerland, 2011. Available from: https://abfit.org.br/images/artigos/16%20-%20WHO%20The%20World%20Medicines%20Situation%202011.pdf. (Accessed 1 July 2022).

[9] F.A. Ripa, M.J. Hossain, M.L. Nesa, M.S. Zahan, S. Mitra, M.A. Rashid, A. Roy, M. Almehmadi, O. Abdulaziz, Phytochemical and pharmacological profiling of buch. Ham. Deciphered thrombolytic, antiarthritic, anthelmintic, and insecticidal potentialities via in vitro approach, Evid. Complement. Alter. Med. (2022), 2594127, https://doi.org/10.1155/2022/2594127.

[10] L. Tripathi, J.N. Tripathi, Role of biotechnology in medicinal plants, Trop J Pharm Res 2 (2) (2003) 243–253.

[11] C. Mesa, O. Ranalison, L.N. Randriantseheno, G. Risuleo, Natural products from Madagascar, socio-cultural usage, and potential applications in advanced biomedicine: a concise review, Molecules 26 (2021) 4507, https://doi.org/10.3390/molecules26154507.

[12] A. Sultana, M.J. Hossain, M.R. Kuddus, M.A. Rashid, M.S. Zahan, S. Mitra, A. Roy, S. Alam, M.M.R. Sarker, I. Naina Mohamed, Ethnobotanical uses, phytochemistry, toxicology, and pharmacological properties of *Euphorbia neriifolia* linn. Against infectious diseases: a comprehensive review, Molecules 27 (2022) 4374, https://doi.org/10.3390/molecules27144374.

[13] H.O. Edeoga, D.E. Okwu, B.O. Mbaebie, Phytochemical constituents of some Nigerian medicinal plants, Afr. J. Biotechnol. 4 (7) (2005) 685–688.

[14] J.A. Chowdhury, M.S. Islam, S.K. Asifuzzaman, M.K. Islam, Antibacterial and cytotoxic activity screening of leaf extracts of *Vitex negundo* (Fam: verbenaceae), J Pharm Sci Res 1 (4) (2009) 103–108.

[15] R. Das, S. Mitra, A.M. Tareq, T.B. Emran, M.J. Hossain, A.M. Alqahtani, Y. Alghazwani, K. Dhama, J. Simal-Gandara, Medicinal plants used against hepatic disorders in Bangladesh: a comprehensive review, J. Ethnopharmacol. 282 (2021), 114588, https://doi.org/10.1016/j.jep.2021.114588.

[16] H. Sies, V.V. Belousov, N.S. Chandel, M.J. Davies, D.P. Jones, G.E. Mann, M.P. Murphy, M. Yamamoto, C. Winterbourn, Defining roles of specific reactive oxygen species (ROS) in cell biology and physiology, Nat. Rev. Mol. Cell Biol. 23 (2022) 499–515, https://doi.org/10.1038/s41580-022-00456-z.

[17] H. Sies, Oxidative stress: a concept in redox biology and medicine, Redox Biol. 4 (2015) 180–183, https://doi.org/10.1016/j.redox.2015.01.002.

[18] D. Nolfi-Donegan, A. Braganza, S. Shiva, Mitochondrial electron transport chain: oxidative phosphorylation, oxidant production, and methods of measurement, Redox Biol. 37 (2020), 101674, https://doi.org/10.1016/j.redox.2020.101674.

[19] A. Ahangarpour, M. Sayahi, M. Sayahi, The antidiabetic and antioxidant properties of some phenolic phytochemicals: a review study, Diabetes Metab. Syndr. 13 (2019) 854–857, https://doi.org/10.1016/j.dsx.2018.11.051.

[20] Y.J. Zhang, R.Y. Gan, S. Li, Y. Zhou, A.N. Li, D.P. Xu, H.B. Li, Antioxidant phytochemicals for the prevention and treatment of chronic diseases, Molecules 20 (2015) 21138–21156, https://doi.org/10.3390/molecules201219753.

[21] A.M. Pisoschi, A. Pop, C. Cimpeanu, G. Predoi, Antioxidant capacity determination in plants and plant-derived products: a review, Oxid. Med. Cell. Longev. 2016 (2016), 9130976, https://doi.org/10.1155/2016/9130976.

[22] F.J. Pashkow, Oxidative stress and inflammation in heart disease: do antioxidants have a role in treatment and/or prevention? Int. J. Inflamm. (2011), 514623 https://doi.org/10.4061/2011/514623, 2011.

[23] P.R. Moreno, V. Fuster, New aspects in the pathogenesis of diabetic atherothrombosis, J. Am. Coll. Cardiol. 44 (12) (2004) 2293–2300, https://doi.org/10.1016/j.jacc.2004.07.060.

[24] A. Mantovani, P. Allavena, A. Sica, F. Balkwill, Cancer-related inflammation, Nature 454 (7203) (2008) 436–444, https://doi.org/10.1038/nature07205.

[25] E.M. Conner, M.B. Grisham, Inflammation, free radicals, and antioxidants, Nutrition 12 (4) (1996) 274–277, https://doi.org/10.1016/s0899-9007(96)00000-8.

[26] Y.Z. Liu, Y.X. Wang, C.L. Jiang, Inflammation: the common pathway of stress-related diseases, Frontiers in human neuroscience 11 (2017) 316, https://doi.org/10.3389/fnhum.2017.00316.

[27] H.R.A. El-Mageed, D.A. Abdelrheem, M.O. Rafi, M.T. Sarker, K. Al-Khafaji, M.J. Hossain, R. Capasso, T.B. Emran, Silico evaluation of different flavonoids from medicinal plants for their potency against SARS-CoV-2, in: Biologics, vol. 1, 2021, pp. 416–434, https://doi.org/10.3390/biologics1030024, 3.

[28] T.E. Tallei, Fatimawali, A.A. Adam, M.M. Elseehy, A.M. El-Shehawi, E.A. Mahmoud, A.D. Tania, N.J. Niode, D. Kusumawaty, S. Rahimah, et al., Fruit bromelain-derived peptide potentially restrains the attachment of SARS-CoV-2 variants to hACE2: a pharmacoinformatics approach, Molecules 27 (2022) 260, https://doi.org/10.3390/molecules27010260.

[29] L. Zhao, H.L. Ciallella, L.M. Aleksunes, H. Zhu, Advancing computer-aided drug discovery (CADD) by big data and data-driven machine learning modeling, Drug Discov. Today 25 (9) (2020) 1624–1638, https://doi.org/10.1016/j.drudis.2020.07.005.

[30] I.A. Guedes, C.S. de Magalhães, L.E. Dardenne, Receptor-ligand molecular docking, Biophysical reviews 6 (1) (2014) 75–87, https://doi.org/10.1007/s12551-013-0130-2.

[31] S. Tafur, J.D. Nelson, D.C. Delong, G.H. Svoboda, Antiviral components of *Ophiorrhiza mungos* and isolation of camptothecin and 10-methoxy camptothecin, Lloydia 39 (4) (1976) 261–262.

[32] A. Jayadev, S. Sari, G.M. Nair, Phytochemical analysis and evaluation of antibacterial and antioxidant activities of *Vitex negundo* and *Ophiorrhiza mungos*, The Biosean 8 (2) (2013) 661–664.

[33] G. Krishnakumar, K.B. Rameshkumar, P. Srinivas, K. Satheeshkumar, P.N. Krishnan, Estimation of camptothecin and pharmacological evaluation of *Ophiorrhiza prostrata* D. Don and *Ophiorrhiza mungos* L, Asian Pac. J. Trop. Biomed. 2 (2) (2012) 727–731.

[34] P.S. Kaushik, M.K. Swamy, S. Balasubramanya, M. Anuradha, Rapid plant regeneration, analysis of genetic fidelity and camptothecin content of micropropagated plants of *Ophiorrhiza mungos* Linn. - a potent anticancer plant, J Crop Sci Biotechnol 18 (2015) 1–8.

[35] D. Arbain, L.T. Byrne, N. Evrayoza, M.V. Sargent, Bracteatine, a quaternary glucoalkaloid from *Ophiorrhiza bracteata*, Aust. J. Chem. 50 (11) (1997) 1111–1112.

[36] N.P. Singh, K.P. Singh, D.K. Singh, Flora of Mizoram, vol. 1, Botanical Survey of India, Calcutta, 2002.

[37] A.A. Mamun, S.M.Z. Hasan, M.S. Islam, M.S. Uddin, M.S. Hosan, T. Rahman, A. Ahmed, Investigation of in-vivo analgesic, anti-diarrheal and CNS activity of ethanolic extracts of *Psychotria silhetensis* leaves, Int J Innov Pharm Sci Res 5 (5) (2017) 48–61.

[38] I.J. Bulbul, U.S. Joty, R. Ahamed, M.R. Haque, M.A. Rashid, Hypoglycemic and hypolipidemic activities of Psychotria sylhetensis hook in alloxan-induced type 2 diabetic rats, BPJ 22 (1) (2019) 41–44.

[39] O.C. Nivea, F.P. MeriEmili, D.R. Suelem, C.M.B. Marcela, F.B. Antonio, C.M.Y. Maria, S.B. Vanderlan, C.P. Angelo, The genus *Psychotria*: phytochemistry, chemotaxonomy, ethnopharmacology and biological properties, J. Braz. Chem. Soc. 27 (8) (2016).

[40] N. Anjum, M.J. Hossain, M.R. Haque, A. Chowdhury, M.A. Rashid, M.R. Kuddus, Phytochemical investigation of schleichera oleosa (lour.) oken leaf, Bangladesh Pharmaceutical Journal 24 (1) (2021 Jan 25) 33–36.

[41] B.C. VenWagenen, R. Larsen, J.H.I.I. Cardellina, D. Randazzo, Z.C. Lidert, C. Swithenbank, Ulosantoin, a potent insecticide from the sponge *Ulosareutzleri*, J. Org. Chem. 58 (1993) 335–337.

[42] C.J. Aiba, R.G.C. Correat, O.R. Gottlieb, Natural occurrence of erdtman's dihydrodiisoeugenol, Phytochemistry 12 (1973) 1163–1164.

[43] V.S.P. Chaturvedula, I. Prakash, Isolation of stigmasterol and sitosterol from the dichloromethane extract of *Rubussua vissimus*, Int. Curr. Pharmaceut. J. 1 (9) (2012) 239–242.

[44] B.N. Meyer, N.R. Ferrigni, J.E. Putnam, J.B. Jacobsen, D.E. Nichols, J.L. McLaughlin, Brine shrimp: a convenient general bioassay for active plant constituents, Planta Med. 45 (1982) 31–34.

[45] N. Anjum, M.J. Hossain, F. Aktar, M.R. Haque, M.A. Rashid, R. Kuddus, Potential in vitro and in vivo bioactivities of Schleichera oleosa (lour.) oken: a traditionally important medicinal plant of Bangladesh, Res. J. Pharm. Technol. 15 (1) (2022) 113–121.

[46] M. Rahman, A. Khatun, M.M. Islam, M.N. Akter, S.A. Chowdhury, M.A.A. Khan, M.I.Z. Shahid, A.A. Rahman, Evaluation of antimicrobial, cytotoxic, thrombolytic, diuretic properties and total phenolic content of *Cinnamomum tamala*, Int. J. Green Pharm. 7 (2013) 236–243.

[47] U.A. Shinde, A.S. Phadke, A.M. Nair, A.A. Mungantiwar, V.J. Dikshit, M.N. Saraf, Membrane stabilizing activity: a possible mechanism of action for the anti-inflammatory activity of *Cedrus deodara* wood oil, Fitoterapia 70 (1999) 251–257.

[48] W. Brand-Williams, M.E. Cuvelier, C. Berset, Use of free radical method to evaluate anti-oxidant activity, Lebensm. Wiss. Technol. 28 (1995) 25–30.

[49] A.L. Barry, in: Lea, Fabager (Eds.), Principle & Practice of Microbiology, third ed., 1976, pp. 21–25. Philadelphia.

[50] A.W. Bayer, W.M. Kirby, J.C. Sherris, M. Turck, Antibiotic susceptibility testing by a standardized single disc method, Am. J. Clin. Pathol. 45 (4) (1966) 493–496.

[51] S. Dallakyan, A.J. Olson, Small-molecule library screening by docking with PyRx, Methods Mol. Biol. 1263 (2015) 243–250, https://doi.org/10.1007/978-1-4939-2269-7_19.

[52] M.J. Hossain, M.Z. Sultan, M.A. Rashid, M.R. Kuddus, Interactions of linagliptin, rabeprazole sodium, and their formed complex with bovine serum albumin: computational docking and fluorescence spectroscopic methods, Anal. Sci. Advan 2 (2021) 480–494.

[53] M.J. Hossain, M.S. Islam, S. Shahriar, S. Sanam, T.B. Emran, C.S. Khatun, M.R. Islam, S. Mitra, K. Dhama, Comedication of rabeprazole sodium causes potential drug-drug interaction with diabetic drug linagliptin: in-vitro and in-silico approaches, J. Exp. Biol. Agric. Sci 9 (2021) 528–542.

[54] T. Jannat, M.J. Hossain, A.M. El-Shehawi, M.R. Kuddus, M.A. Rashid, S. Albogami, I. Jafri, M. El-Shazly, M.R. Haque, Chemical and pharmacological profiling of *Wrightia coccinea* (roxb. Ex hornem.) sims focusing antioxidant, cytotoxic, antidiarrheal, hypoglycemic, and analgesic properties, Molecules 27 (2022) 4024, https://doi.org/10.3390/molecules27134024.

[55] M.J. Hossain, M.A. Rashid, M.Z. Sultan, Transition metal chelation augments the half-life of secnidazole: molecular docking and fluorescence spectroscopic approaches, Drug Res. 70 (2020) 583–592, https://doi.org/10.1055/a-1252-2322.

[56] Z. Bikadi, E. Hazai, Application of the PM6 semi-empirical method to modeling proteins enhances docking accuracy of AutoDock, J. Cheminformat. 1 (2009) 1–6.

[57] M.C.S. Khatun, M.A. Muhit, M.J. Hossain, M.A. Al-Mansur, S.M.A. Rahman, Isolation of phytochemical constituents from *Stevia rebaudiana* (Bert.) and evaluation of their anticancer, antimicrobial and antioxidant properties via *in vitro* and *in silico* approaches, Heliyon 26 (7) (2021), e08475, https://doi.org/10.1016/j.heliyon.2021.e08475.

[58] W. Kaplan, T.G. Littlejohn, Swiss-PDB viewer (deep view), Briefings Bioinf. 2 (2001) 195–197, https://doi.org/10.1093/bib/2.2.195.

[59] S. Ekins, J. Mestres, B. Testa, In silico pharmacology for drug discovery: methods for virtual ligand screening and profiling, Br. J. Pharmacol. 152 (2007) 9–20, https://doi.org/10.1038/sj.bjp.0707305.

[60] D.E. Pires, T.L. Blundell, D.B. Ascher, pkCSM: predicting small-molecule pharmacokinetic and toxicity properties using graph-based signatures, J. Med. Chem. 58 (9) (2015) 4066–4072.

[61] F. Kandsi, A. Elbouzidi, F.Z. Lafdil, N. Meskali, A. Azghar, M. Addi, C. Hano, A. Maleb, N. Gseyra, Antibacterial and antioxidant activity of Dysphania ambrosioides (L.) mosyakin and clemants essential oils: experimental and computational approaches, Antibiotics 11 (4) (2022) 482.

[62] F. Kandsi, F.Z. Lafdil, A. Elbouzidi, S. Bouknana, A. Miry, M. Addi, R. Conte, C. Hano, N. Gseyra, Evaluation of acute and subacute toxicity and LC-MS/MS compositional alkaloid determination of the hydroethanolic extract of dysphania ambrosioides (L.) mosyakin and clemants flowers, Toxins 14 (7) (2022) 475.

[63] OECD, Test No. 423, *Acute Oral Toxicity - Acute Toxic Class Method*, OECD Guidelines for the Testing of Chemicals, Section, vol. 4, OECD Publishing, Paris, 2002, https://doi.org/10.1787/9789264071001-en.

[64] A. Daina, V. Zoete, A BOILED-egg to predict gastrointestinal absorption and brain penetration of small molecules, ChemMedChem 11 (11) (2016) 1117–1121, https://doi.org/10.1002/cmdc.201600182.

[65] S. Mitra, M.S. Lami, T.M. Uddin, R. Das, F. Islam, J. Anjum, M.J. Hossain, T.B. Emran, Prospective multifunctional roles and pharmacological potential of dietary flavonoid narirutin, Biomed. Pharmacother. 150 (2022), 112932, https://doi.org/10.1016/j.biopha.2022.112932.

[66] S. Mitra, M. Muni, N.J. Shawon, R. Das, T.B. Emran, R. Sharma, et al., Tacrine derivatives in neurological disorders: focus on molecular mechanisms and neurotherapeutic potential", Oxid. Med. Cell. Longev. 2022 (2022), https://doi.org/10.1155/2022/7252882. Article ID 7252882, 22 pages, 2022b.

[67] J. Anjum, S. Mitra, R. Das, R. Alam, A. Mojumdar, T.B. Emran, et al., A renewed concept on the MAPK signaling pathway in cancers: polyphenols as a choice of therapeutics, Pharmacol. Res. (2022), 106398, https://doi.org/10.1016/j.phrs.2022.106398.

[68] J. Zhang, H. Si, K. Lv, Y. Qiu, J. Sun, Y. Bai, B. Li, X. Zhou, J. Zhang, Licarin-B exhibits activity against the *Toxoplasma gondii* RH strain by damaging mitochondria and activating autophagy, Front. Cell Dev. Biol. 9 (2021), 684393, https://doi.org/10.3389/fcell.2021.684393.

[69] H. Bae, G. Song, W. Lim, Stigmasterol causes ovarian cancer cell apoptosis by inducing endoplasmic reticulum and mitochondrial dysfunction, Pharmaceutics 12 (6) (2020) 488, https://doi.org/10.3390/pharmaceutics12060488.

[70] H. Ali, S. Dixit, D. Ali, S.M. Alqahtani, S. Alkahtani, S. Alarifi, Isolation and evaluation of anticancer efficacy of stigmasterol in a mouse model of DMBA-induced skin carcinoma, Drug Des. Dev. Ther. 9 (2015) 2793–2800, https://doi.org/10.2147/DDDT.S83514.

[71] R. Pratiwi, C. Nantasenamat, W. Ruankham, W. Suwanjang, V. Prachayasittikul, S. Prachayasittikul, K. Phopin, Mechanisms and neuroprotective activities of stigmasterol against oxidative stress-induced neuronal cell death *via* sirtuin family, Front. Nutr. 8 (2021), 648995, https://doi.org/10.3389/fnut.2021.648995.

[72] T. Kangsamaksin, S. Chaithongyot, C. Wootthichairangsan, R. Hanchaina, C. Tangshewinsirikul, J. Svasti, Lupeol and stigmasterol suppress tumor angiogenesis and inhibit cholangiocarcinoma growth in mice via downregulation of tumor necrosis factor-α, PLoS One 12 (12) (2017), e0189628 https://doi.org/10.1371/journal.pone.0189628.

[73] Y.S. Kim, X.F. Li, K.H. Kang, B. Ryu, S.K. Kim, Stigmasterol isolated from marine microalgae Navicula incerta induces apoptosis in human hepatoma HepG2 cells, BMB reports 47 (8) (2014) 433–438, https://doi.org/10.5483/bmbrep.2014.47.8.153.

[74] Z. Memariani, R. Moeini, S.S. Hamedi, N. Gorji, S.A. Mozaffarpur, Medicinal plants with antithrombotic property in Persian medicine: a mechanistic review, J. Thromb. Thrombolysis 45 (1) (2018) 158–179, https://doi.org/10.1007/s11239-017-1580-3.

[75] N. Gupta, Y.Y. Zhao, C.E. Evans, The stimulation of thrombosis by hypoxia, Thromb. Res. 181 (2019) 77–83, https://doi.org/10.1016/j.thromres.2019.07.013.

[76] A.J. Chakraborty, T.M. Uddin, B. Matin Zidan, S. Mitra, R. Das, F. Nainu, K. Dhama, A. Roy, M.J. Hossain, A. Khusro, T.B. Emran, *Allium cepa*: a treasure of bioactive phytochemicals with prospective Health benefits, in: Evidence-based Complementary and Alternative Medicine, eCAM, 2022, 4586318, https://doi.org/10.1155/2022/4586318, 2022.

[77] V.J. Marder, Recombinant streptokinase: opportunity for an improved agent, Blood Coagul. Fibrinolysis 4 (1993) 1039–1040.
[78] D.H. Wu, G.Y. Shi, W.J. Chuang, J.M. Hsu, K.C. Young, C.W. Chang, Coiled coil region of streptokinase gamma-domain is essential for plasminogen activation, J. Biol. Chem. 276 (2001) 15025–15033.
[79] W. Qu, J. Xue, F.H. Wu, J.Y. Liang, Lignans from Saururus chinensis with antiplatelet aggregation and neuroprotective activities, Chemistry of natural compounds 50 (5) (2014 Nov) 814–818.
[80] J. Omale, P.N. Okafor, Comparative anti-oxidant capacity, membrane stabilization, polyphenol composition and cytotoxicity of the leaf and stem of *Cissus multistriata*, Afr. J. Biotechnol. 7 (2008) 3129–3133.
[81] Noor-E-Tabassum, R. Das, M.S. Lami, A.J. Chakraborty, S. Mitra, T.E. Tallei, R. Idroes, A.A. Mohamed, M.J. Hossain, K. Dhama, G. Mostafa-Hedeab, T.B. Emran, *Ginkgo biloba*: a treasure of functional phytochemicals with multimedicinal applications, Evid. base Compl. Alternative Med.: eCAM 2022 (2022), 8288818, https://doi.org/10.1155/2022/8288818.
[82] S. Sarwar, M.J. Hossain, N.M. Irfan, T. Ahsan, M.S. Arefin, A. Rahman, A. Alsubaie, B. Alharthi, M.U. Khandaker, D.A. Bradley, T.B. Emran, S.N. Islam, Renoprotection of selected antioxidant-rich foods (water spinach and red grape) and probiotics in gentamicin-induced nephrotoxicity and oxidative stress in rats, Life 12 (1) (2022) 60, https://doi.org/10.3390/life12010060.
[83] G.K. Jayaprakasha, R.L. Jaganmohan, Phenolic constituents from lichen *Parmontrema stuppeum*, Hale and anti-oxidant activity 56 (2000) 1018–1022.
[84] N. Ito, M. Hiroje, G. Fukusina, H. Tauda, T. Shira, M. Tatematsu, Studies on anti-oxidants, their carcinogenic and modifying effects on chemical carcinogenesis, Food Chem. Toxicol. 24 (1986) 1071–1081.
[85] H.P. Wichi, Enhanced tumor development by butylated hydroxyanisole (BHA) from the prosecretive of effects of forestomach and oesophageal squmous epithelium, Food Chem. Toxicol. 26 (1988) 717–723.
[86] J.P. Hou, H. Wu, Y. Wang, X.C. Weng, Isolation of some compounds from nutmeg and their antioxidant activities, Czech J. Food Sci. 30 (2) (2012 Mar 9) 164–170.
[87] S. Panda, M. Jafri, A. Kar, B.K. Meheta, Thyroid inhibitory, antiperoxidative and hypoglycemic effects of stigmasterol isolated from Butea monosperma, Fitoterapia 80 (2) (2009) 123–126, https://doi.org/10.1016/j.fitote.2008.12.002.
[88] Q. Liang, J. Yang, J. He, X. Chen, H. Zhang, M. Jia, K. Liu, C. Jia, Y. Pan, J. Wei, Stigmasterol alleviates cerebral ischemia/reperfusion injury by attenuating inflammation and improving antioxidant defenses in rats, Biosci. Rep. 40 (4) (2020), BSR20192133, https://doi.org/10.1042/BSR20192133.
[89] T.M. Uddin, A.J. Chakraborty, A. Khusro, B. Zidan, S. Mitra, T.B. Emran, K. Dhama, M. Ripon, M. Gajdács, M. Sahibzada, M.J. Hossain, N. Koirala, Antibiotic resistance in microbes: history, mechanisms, therapeutic strategies and future prospects, Journal of infection and public health 14 (12) (2021) 1750–1766, https://doi.org/10.1016/j.jiph.2021.10.020.
[90] R. Das, A. Rauf, S. Mitra, T.B. Emran, M.J. Hossain, Z. Khan, S. Naz, B. Ahmad, A. Meyyazhagan, K. Pushparaj, C.C. Wan, B. Balasubramanian, K.R. Rengasamy, J. Simal-Gandara, Therapeutic potential of marine macrolides: an overview from 1990 to 2022, Chem. Biol. Interact. 365 (2022), 110072, https://doi.org/10.1016/j.cbi.2022.110072. Advance online publication.
[91] G. Kapoor, S. Saigal, A. Elongavan, Action and resistance mechanisms of antibiotics: a guide for clinicians, J. Anaesthesiol. Clin. Pharmacol. 33 (3) (2017) 300–305, https://doi.org/10.4103/joacp.JOACP_349_15.
[92] M.M. Mailafiya, A.J. Yusuf, M.I. Abdullahi, G.A. Aleku, I.A. Ibrahim, M. Yahaya, H. Abubakar, A. Sanusi, H.W. Adamu, C.O. Alebiosu, Antimicrobial activity of stigmasterol from the stem bark of Neocarya macrophylla, Journal of Medicinal Plants for Economic Development 2 (1) (2018 Apr 25) 1–5.
[93] M.C. Sanguinetti, M. Tristani-Firouzi, hERG potassium channels and cardiac arrhythmia, Nature 440 (7083) (2006) 463–469.
[94] S. Kalyaanamoorthy, K.H. Barakat, Development of safe drugs: the hERG challenge, Med. Res. Rev. 38 (2) (2018) 525–555.
[95] L. Chedik, D. Mias-Lucquin, A. Bruyere, O. Fardel, In silico prediction for intestinal absorption and brain penetration of chemical pesticides in humans, Int. J. Environ. Res. Publ. Health 14 (7) (2017 Jul) 708.